

Overexpression of Fibroblast Activation Protein (FAP) in stroma of proliferative inflammatory atrophy (PIA) and primary adenocarcinoma of the prostate

Fernanda Caramella-Pereira¹, Qizhi Zheng¹, Jessica L. Hicks¹, Sujayita Roy, Tracy Jones¹, Martin Pomper⁵, Lizamma Antony³, Alan K. Meeker², Srinivasan Yegnasubramanian⁴, Angelo M. De Marzo^{*2}, W. Nathaniel Brennen^{*3}

¹ Department of Pathology, Johns Hopkins University School of Medicine, Baltimore, MD,

² Department of Pathology, Oncology, and Urology, The Sidney Kimmel Comprehensive Cancer Center at Johns Hopkins and the James Buchanan Brady Urological Research Institute., Baltimore, MD,

³ Department of Oncology, and Urology, The Sidney Kimmel Comprehensive Cancer Center at Johns Hopkins and the James Buchanan Brady Urological Research Institute., Baltimore, MD

⁴ Department of Pathology, Oncology, and Urology, The Sidney Kimmel Comprehensive Cancer Center at Johns Hopkins and the James Buchanan Brady Urological Research Institute, Baltimore, MD

⁵ University of Texas, Southwestern Medical Center, Dallas, TX

*indicate co-senior authors

Address for correspondence: A M De Marzo, MD, Department of Pathology, 1550 Orleans Street. CRB2, Rm144, Baltimore, Maryland, 410 614 5686 Main, 410 502 9817 Fax

INCREASED FAP IN PIA AND PROSTATE CANCER

Abstract:

Fibroblast activation protein (FAP) is a serine protease upregulated at sites of tissue remodeling and cancer that represents a promising therapeutic and molecular imaging target. In prostate cancer, studies of FAP expression using tissue microarrays are conflicting, such that its clinical potential is unclear. Furthermore, little is known regarding FAP expression in benign prostatic tissues. Here we demonstrated, using a novel iterative multiplex IHC assay in standard tissue sections, that FAP was nearly absent in normal regions, but was increased consistently in regions of proliferative inflammatory atrophy (PIA). In carcinoma, FAP was expressed in all cases, but was highly heterogeneous. High FAP levels were associated with increased pathological stage and cribriform morphology. We verified that FAP levels in cancer correlated with CD163+ M2 macrophage density. In this first report to quantify FAP protein in benign prostate and primary tumors, using standard large tissue sections, we clarify that FAP is present in all primary prostatic carcinomas, supporting its potential clinical relevance. The finding of high levels of FAP within PIA supports the injury/regeneration model for its pathogenesis and suggests that it harbors a protumorigenic stroma. Yet, high levels of FAP in benign regions could lead to false positive FAP-based molecular imaging results in clinically localized prostate cancer.

INCREASED FAP IN PIA AND PROSTATE CANCER

Introduction

Fibroblast activation protein (FAP) is a type II transmembrane serine protease with both endopeptidase and dipeptidyl peptidase (DPP) activities.¹⁻³ FAP expression is generally absent in normal tissues but is upregulated at sites of tissue remodeling during wound healing, in regions of fibrosis and in many invasive cancers.^{1,3-5} FAP has been implicated in cancer initiation and progression by promoting tumor cell proliferation, angiogenesis, stromal invasion and immune suppression.^{1,3,6} As a result, FAP protease activity has emerged as a molecular imaging target in cancer⁷⁻⁹ and as a potential anti-cancer drug target.^{1,10} In addition, FAP activity is a promising target for prodrugs designed to be activated in regions of high FAP expression.^{11,12}

In prostate cancer there are conflicting studies regarding FAP expression.^{9,13-16} Using multiplex immunofluorescence on tissue microarrays (TMAs), increasing FAP levels have been positively associated with higher Gleason score, MRI positivity, biochemical recurrence, and disease progression after prostatectomy.¹⁶ However, a separate recent study found no FAP protein expression in primary tumors using TMAs, but noted high levels of expression in metastatic castration resistant prostate cancer (mCRPC).¹³ Furthermore, while FAP mRNA has been examined in relation to cribriform morphology,^{15,17} FAP protein expression has not been systematically characterized in relation to morphological features of disease aggressiveness beyond Gleason grading in primary prostate carcinoma. Finally, while FAP expression was found to be increased in a region of inflammation in benign prostatic hyperplasia (BPH) in a single case,⁹ its expression in benign prostatic tissues has been reported as negative or has not been commented upon and it has not been systematically studied in benign inflammatory lesions of the prostate.^{9,13-16}

The lack of information regarding FAP expression in benign prostate tissues represents an important knowledge gap regarding both prostatic carcinogenesis and FAP imaging and theranostics. For example, non-cancerous regions in the prostate contain foci of inflammation, epithelial cell injury, and proliferation, referred to as proliferative inflammatory atrophy (PIA). To date, FAP expression has not been examined in these lesions. These foci have been proposed as precursor lesions for the development of high grade prostatic intraepithelial neoplasia (PIN) and/or invasive adenocarcinoma.¹⁸⁻²⁰ Also, most studies of PIA have focused on the epithelial cells. For example, in addition to an increased proliferative fraction, intermediate luminal cells in PIA show increased expression of *GSTP1* and *BCL-2*,²¹ *GSTA1*,²² *Keratin 5*,²³ *PTGS2*,^{24,25} and lactoferrin (LTF).²⁶ Luminal intermediate cells in PIA also show decreased expression of *CD38*,²⁷ rare *GSTP1* methylation,^{28,29} rare *TMPRSS2-ERG* gene fusions,³⁰ as well as increased expression of genes indicative of immune activation, some of which have overlap with those seen in lung club cells.^{31,32} These findings provide strong evidence that many luminal epithelial cells in PIA are experiencing a stress response, and/or immune activation response, yet no previous studies have focused on the stromal compartment in PIA where FAP would be expected to be expressed. It is also important to evaluate the expression pattern and levels of FAP in non-neoplastic prostatic tissues, since the presence of high levels of FAP in such benign regions could lead to false positive FAP-based molecular imaging results. To address these

INCREASED FAP IN PIA AND PROSTATE CANCER

unresolved questions in a spatially relevant and quantitative manner, we developed a novel quantitative chromogenic multiplex IHC assay centered around a highly analytically validated FAP antibody for IHC. Since FAP expression tends to be heterogeneous, we used whole slide tissue sections from radical prostatectomy specimens to avoid under sampling of tissue that may occur using TMAs.

Materials and Methods

Patient Samples

Formalin fixed and paraffin embedded (FFPE) prostate tissue sections were obtained from The Johns Hopkins Hospital department of pathology from radical prostatectomy specimens from men treated for clinically localized prostatic adenocarcinoma. The use of these tissues was approved by the Johns Hopkins University School of Medicine Institutional Review Board (NA_00087094). Prostatectomy specimens were handled as previously described.³³ For each case (N=56), a single FFPE block was selected representing the highest grade tumor. The Gleason grade groups of the retrieved cases ranged from GG1 to GG5, and the pathological stages ranged from organ confined (T2,N0) to pelvic lymph node metastasis (any T, N1) (**Table 1**).

IHC

Antibodies used in this study included those against FAP, CD45, CD163, p63, Keratin 8 (CK8), desmin, CD31, vimentin, s100 and alpha smooth muscle actin; the details and conditions are presented in **Supplemental Table 1**. Each antibody was optimized by individual single-plex staining before being incorporated into the iterative multiplex IHC assay as described.³³ These antibodies were combined in two different panels using a multiplex approach that entails chromogenic IHC staining followed by whole slide scanning, chromogen and antibody stripping, and then iterating with the next antibody and cycle.

Slides were scanned using a 40x objective on a Roche/Ventana DP200. Whole slide images (WSIs) from each staining round were uploaded to the HALO image analysis platform (Indica Labs), and processed by color deconvolution, image registration and image fusion as described.³³ CK8 staining was used to facilitate training of a random forest classifier to determine epithelial and stromal areas in regions of tumor as described.³³ HALO Area Quantification (Area Quantification FL v2.3.4) tools were used to determine areas of positive staining for FAP, CD163 and for CD45.

Quantification

Regions of normal appearing epithelium and stroma, PIA and invasive adenocarcinoma were annotated on whole slide images of H&E stained sections. For quantifying FAP, we used two separate threshold cutoffs for positive pixels. The lower cutoff was used to identify all positive staining above background and the higher cutoff was used to only quantify high intensity areas of FAP. For each of these thresholds, we defined the percent area of FAP staining (FAP Area Fraction) as the percentage of the FAP positive pixel counts divided by the total pixel counts in the annotated total area. The total tumor area, consisting of both tumor epithelium and tumor stroma, was defined by manual annotation of tumor regions, excluding benign glands and after subtracting lumens and empty spaces. The percent stromal area of FAP staining (FAP Stroma Area Fraction) was defined as the percentage of area of FAP positive pixel counts divided by the total stromal area. In general, both of these FAP threshold measurements provided similar trends overall and the results correlated with each other.

INCREASED FAP IN PIA AND PROSTATE CANCER

For quantification of M2 macrophages, we used the positive pixel counts of the CD163 area to generate a CD163 Area Fraction and CD163 Stroma Area Fraction for each case as above. For total leukocytes, we used the positive pixel counts of the CD45 area to generate a CD45 Area Fraction and CD45 Stroma Area Fraction.

In Situ Hybridization for FAP

RNA in situ hybridization (RISH) was performed using the RNAscope 2.5 FFPE Brown Reagent Kit (Advanced Cell Diagnostics, Inc.) largely as previously described.³⁴ Briefly, FFPE cell line slides were baked at 60°C for 30 minutes followed by deparaffinization in 100% xylene twice for 5 minutes each and two changes of 100% alcohol. The slides were treated with endogenous peroxidase-blocking pretreatment reagent and then incubated for 18 minutes in a boiling water bath and then treated with protease digestion buffer for 20 minutes at 40°C. The slides were incubated with ACD RNAscope target probe set Cat No. 411971, NCBI reference accession No. NM_004460.2, target region (Base pairs: 486-1588) for 2 hours at 40°C, followed by signal amplification. DAB was used for colorimetric detection for 10 minutes at room temperature.

hPrCSC-44c immortalization

PrCSC-44c were obtained from radical prostatectomy tissue as previously described.³⁵ PrCSC-44c was hTERT-immortalized using the pLOX-TERT-iresTK (plasmid #12245, Addgene, Watertown MA) lentiviral vector³⁶ as previously described to generate hPrCSC-44c as a model of prostate cancer-derived stromal cells (MSCs + CAFs).³⁷ Briefly, HEK293T cells were first co-transfected with the TERT-containing vector and packaging plasmid using Lipofectamine 2000 Transfection reagent (Sigma-Aldrich, St. Louis, MO) diluted in Opti-MEM I reduced serum media (Gibco, Waltham, MA). After 24 hours at 37°C, the media was removed and replaced with standard Opti-MEM. The supernatant was collected after an additional 24 hours of incubation at 37°C, and the virus was harvested and concentrated by ultracentrifugation for 2 hours at 100,000 x g. Virus was then added to the PrCSC-44c culture media (hMSC Expansion media, RoosterBio, Frederick, MD) supplemented with 8 mg/mL of polybrene (Sigma-Aldrich) and incubated at 37°C for 24 hours. The virus-containing supernatant was removed and replaced with fresh media. Immortalization was confirmed via continuous passaging of the cells at ~80% confluence in hMSC Expansion media at a 1:5 dilution and the population doublings significantly exceeded those of the non-immortalized parental cells as they underwent senescence under standard tissue culture conditions (18 vs. >30 passages).

Statistical analysis

Statistical analysis was carried out in STATA 18 for Microsoft Windows. Differences in percent FAP area between groups were assessed using the Wilcoxon rank-sum (Mann-Whitney) test for unpaired analyses and the Wilcoxon signed-rank test for paired analyses.

INCREASED FAP IN PIA AND PROSTATE CANCER

Statistical significance was set at $P < 0.05$. Linear regression was used to examine the relationship between the percent FAP area and percent CD163 area and percent CD45 areas.

Results

Analytic Validation of FAP IHC Assay and Multiplex Staining

To analytically validate an IHC assay for FAP, cell lines with known FAP expression were processed by formalin fixation and paraffin embedding (FFPE)³⁸ and stained with an anti-FAP antibody. As a positive control, we used a cell line derived from TERT-immortalized prostate stromal cells (hPrCSC-44c cells) that expresses FAP mRNA and protein,^{12,35} and these cells were positive by IHC (**Fig. 1A**). As an isogenic negative control, hPrCSC-44c cells were subjected to targeted disruption of *FAP* by CRISPR/Cas9. Staining for FAP in these cells was negative (**Fig. 1B**). EnzaR-CWR22Rv1^{39,40} prostate cancer cells do not express FAP mRNA and protein,¹² and they were negative by IHC (**Fig. 1C**) and by *in situ* hybridization for FAP mRNA (**Fig. 1G**). As an additional isogenic control, we transfected a cDNA clone encoding human FAP into EnzaR-CWR22RV1 cells and this resulted in robust anti-FAP immunostaining (**Fig. 1D**) and mRNA expression (**Fig. 1H**). Taken together, these results provide genetic validation of our IHC assay conditions for FAP protein.

To evaluate FAP expression in prostate tissues qualitatively, quantitatively and spatially, we developed a multiplex IHC assay using an iterative chromogenic approach (**Fig. 2; Supplemental Table 1**).^{33,41} An advantage of this iterative method is that each round of IHC is performed as a single-plex stain which facilitates quality control assessments for each individual marker before the next round of staining (**Fig. 2**). Each whole slide image is then subjected to color deconvolution and the pseudo-colored whole slide images from each staining round are fused to generate a multiplex pseudo-multicolored image³³ (**Fig. 2**). To evaluate FAP expression by tissue compartment (e.g., stroma versus epithelial), we used CK8, which stains all prostatic epithelial cells (benign and cancerous).³³ To aid in the determination of benign versus cancerous regions, as well as intraductal carcinoma, the panel also includes the basal cell marker, p63, which is expressed in basal cells outlining all benign glands (including PIA) as well as those containing intraductal carcinoma and prostatic intraepithelial neoplasia (PIN).³³ We included CD163 for M2 macrophages⁴² and CD45 for total immune cells.

FAP in Normal Appearing Regions and PIA

In regions of normal appearing prostatic tissue (without inflammation or atrophy) there was generally a complete absence of FAP staining (**Fig. 3A-B**). Regions of PIA, by contrast, often showed abundant, albeit heterogeneous, FAP staining in the stromal compartment (**Fig. 3D and F**). In some regions of PIA lesions, smooth muscle cells, which occupy the majority of the normal prostatic stroma area, were replaced by fibrosis (**Fig. 3E-F**), and these and surrounding areas generally showed high levels of FAP staining (**Fig. 3F**). PIA lesions often contain corpora amylacea, and often the most intense FAP staining was present in the stromal regions directly abutting these structures (**Fig. 3C-D and Fig. 5B**)

FAP in Prostatic Adenocarcinoma

In primary adenocarcinoma lesions, FAP staining was positive in all cases (N=56). Except for very focal staining in a small fraction of tumor cells in a single case, FAP was exclusively localized to the stromal compartment. Strikingly, in most cases, the extent and intensity of FAP staining was highly heterogeneous, often with some regions showing very high levels of staining and others containing much lower levels (**Fig. 4**).

Primary prostatic adenocarcinomas often contain malignant glands infiltrating between and around nearby benign glands. In tumors characterized by this growth pattern, the highest levels of FAP staining generally occurred directly surrounding benign atrophic glands of PIA (**Fig. 5**).

In carcinoma lesions with cribriform or intraductal architecture, FAP staining was not present within the tumor cell epithelial nodules, but was commonly present, often at high levels, in the stroma directly abutting the perimeter of these structures (**Fig. 6**), which is similar to that seen recently for FAP mRNA localization.¹⁵

Quantitative Image Analysis Comparing Normal PIA and Carcinoma Regions

We next quantified the area of FAP staining in the different tissue types encompassing normal appearing regions, PIA, and invasive adenocarcinomas. For each of these tissue types, we determined the percentage of area occupied by FAP staining in relation to total tissue area as well as to stromal area. To quantify the epithelial and stromal tissue areas separately (as well as the total tissue area), we implemented a random forest classifier using keratin 8 IHC staining as a machine learning training guide³³ (**Fig. 7**). We calculated the percentage area of FAP staining (FAP area fraction) in randomly selected areas from each tissue type where each tissue type was present on the same slides (N=5 matched patient pairs). **Fig. 8 and Table 2** show that the FAP area fraction was extremely low or absent in normal regions, but was increased in regions of PIA (**Fig. 8** shows one spot on each graph per patient after taking the median values and **Supplemental Fig. 1** shows all data points for all individual regions examined). In carcinoma, the FAP area fraction was also increased, compared with normal appearing regions, albeit it was not as high as in PIA. Exploring mRNA expression data from a recent study (The JHU LCM Prostatectomy Dataset) from our group using laser capture microdissection,⁴³ FAP was overexpressed in tumor regions compared with matched normal regions (**Supplemental Fig. 2**). This provides additional evidence for FAP overexpression in primary prostatic adenocarcinoma.

Next, we quantified the area fraction of CD163 positive macrophages and total CD45 positive total immune cells in these same regions. As expected, the area of M2 macrophages and overall immune cells was elevated in PIA as compared with normal appearing regions (**Fig. 8; Supplemental Fig. 1**). Also, both CD163 positive macrophages and total CD45 positive immune cells were elevated in the regions of adenocarcinoma – as compared with normal regions – and were lower than in PIA (**Fig. 8; Supplemental Fig. 1**).

Quantitative Analysis of FAP in Carcinoma in Whole Tumor Regions

We next assessed the FAP area fraction in overall tumor regions for all 56 invasive carcinomas. For this, we annotated and quantified FAP staining within the entire tumor region present on standard whole slides for each case (**Fig. 7** shows an example). We examined FAP levels in relation to Gleason grade groups, pathological stage, and other morphological features (Figure 9, **Tables 3a, 3b and 3c**).

FAP expression in Grade Group 1 tumors (Gleason score 3+3=6) was generally quite low with one exception (**Table 3a, Fig. 9A**). There was a trend of increasing FAP protein levels with increasing grade groups, but this trend was relatively weak and not statistically significant (**Table 3a, Fig. 9A**). A similar trend was seen with CD163 positive macrophage area (**Table 3a, Fig. 9B**).

In terms of pathological stage at prostatectomy, the FAP area fraction was higher in cases with non-organ confined disease (\geq pT3a) versus organ confined (pT2) (**Fig. 9**) and in cases considered high stage (pT3b showing seminal vesicle invasion or Any N1 showing lymph node metastasis) versus lower stages (\leq pT3a) (**Table 3**). The CD163 positive macrophage area fraction, but not CD45 area, was also increased in higher stage cases (**Table 3a; Fig. 9E-F**).

In terms of morphological characteristics not encompassed by Gleason grade groups, we recorded whether carcinoma lesions harbored any reactive stroma in the nearby H&E stained sections and observed a correlation between FAP area fraction and the presence of reactive stroma (**Supplementary Figure 3; Table 3b**). Cribriform architecture is known to be associated with adverse outcomes, independent of Gleason scoring. Furthermore, a recent study found increased FAP mRNA in cribriform prostatic carcinoma.¹⁷ 46.4% of cases showed any cribriform glands; 25% had large cribriform glands. There was increased FAP in cases with any cribriform glands and with large cribriform glands ($P = 0.04$ rank-sum). FAP expression was not, however, associated with the presence of intraductal carcinoma ($N = 13$ cases with intraductal carcinoma, $P = 0.972$, rank-sum).

Prior studies found that FAP mRNA levels correlated with the extent of CD163 mRNA (used as surrogate for M2 macrophage infiltration) across multiple tumor types,⁴⁴ and FAP protein and CD163 protein correlated in primary prostatic adenocarcinomas.¹⁶ In the present study, there was a positive correlation between the FAP area fraction and the CD163 area fraction (**Fig. 10A**). This is despite the fact that there was not an association between FAP area fraction and the extent of infiltration by total CD45 positive immune cells (**Fig. 10B**). There was a trend towards increased CD163 area fraction and Grade Groups, although this was not significant (**Fig. 9B**). In terms of CD45 area fraction, there was an apparent increase in Grade group 3 tumors, yet a somewhat lower level in combined high grade (Grade group 4 and 5) lesions (**Fig. 9C**). We did not observe appreciable colocalization of FAP and CD163, indicating that intratumoral prostatic macrophages generally do not express FAP. Exploring mRNA

INCREASED FAP IN PIA AND PROSTATE CANCER

expression data from the The JHU LCM Prostatectomy Dataset, as well as from a prior microarray study in prostate prostatic adenocarcinomas⁴⁵ and from the TCGA, FAP mRNA correlated with CD163 mRNA in both studies (**Supplemental Fig. 4**).

Relation of FAP Expression to Common Molecular Alterations

A prior study indicated that FAP expression was higher in prostate cancer cases with PTEN loss.¹⁶ Also, 25-50% of prostatic adenocarcinomas harbor ERG gene fusions, which denote a specific molecular subtype. We thus evaluated the level of FAP in relation to the status of PTEN and ERG as characterized by IHC.³³ Although not statistically significant, there was a trend for increased area fraction of FAP staining in cases with PTEN loss as well as in cases that were ERG positive (**Supplemental Fig. 5**). The extent of CD163 positive area fraction was higher in cases with complete PTEN loss (**Supplemental Fig. 5**).

INCREASED FAP IN PIA AND PROSTATE CANCER

Discussion

In this study, we report, for the first time, widespread and high levels of FAP expression within benign prostatic tissues in regions of PIA. Furthermore, our study is the first to use standard whole slides, which provide an advantage by markedly increasing the amount of tumor tissue examined for FAP expression, as compared with TMA spots. Using this approach, FAP protein was detected within the tumor microenvironment in all primary untreated prostatic adenocarcinomas examined. Using whole slides also revealed that FAP expression was generally highly heterogeneous within given tumors, which could in part explain prior discrepant results using TMAs. We validated our staining using genetic controls, which demonstrated very high specificity for FAP protein. Having null cell line controls allowed us to maximize our signal while keeping the noise extremely low, which provided high sensitivity for FAP protein detection. It is likely that this increased our ability to detect relatively low levels of FAP expression.

In addition to shedding light on the pathogenesis of prostate cancer development, the present results also have clinical implications. Molecular imaging and theranostic approaches targeting FAP using recently developed radiopharmaceuticals are proceeding rapidly and are considered highly promising as novel cancer imaging and therapeutic agents.^{1,7-9} Our findings suggest that future applications of molecular imaging targeting FAP, as well as FAP-targeted theranostics, should be considered worth pursuing in clinically localized prostate cancer; yet, at the same time, it is important to recognize that false positive imaging could occur if relatively large regions of FAP-positive PIA are present. Careful tissue mapping with registration between imaging results and histopathologic findings will be required to evaluate this accurately.

In non-neoplastic prostate tissues, we have proposed that in response to infectious agents (*e.g.*, bacteria, fungi, or viruses), inflammatory cell infiltrates, dietary toxicants, urine reflux, *etc.*, prostatic epithelial cells undergo cellular injury and cell death.¹⁸⁻²⁰ Whether initiated by inflammation or otherwise, the cell injury/death would also be expected to further drive inflammation in a feed-forward loop.¹⁹ Further, to restore the barrier function, epithelial regeneration occurs via proliferation of intermediate epithelial cells, which are highly enriched in PIA lesions.^{18-20,28} Here, we provide the first evidence showing that regions of PIA often contain high levels of FAP protein in their stromal microenvironment. In fact, in many of the cases, the highest level of FAP expression occurred in PIA lesions. Along with morphological features showing overt fibrosis, these findings are consistent with the injury-regeneration model of PIA development and adds a new feature consisting of stromal injury. We postulate that this stromal injury occurs from damage to prostatic smooth muscle cells and fibroblasts, along with other elements such as small blood vessels and nerves, by the same mechanisms described above for epithelial cells.

These findings indicate that regions of PIA with increased FAP appear to represent a wound undergoing tissue remodeling, analogous to wounds of the skin and other body sites. The results also suggest a novel concept that those PIA lesions with increased FAP harbor a supportive microenvironment that increases their risk of progressing to PIN and/or adenocarcinoma. We hypothesize that, at times, PIN or early carcinoma lesions that develop in

INCREASED FAP IN PIA AND PROSTATE CANCER

regions of high FAP may harbor a growth advantage due to the known function of FAP in promoting epithelial cell proliferation, new blood vessel formation, stromal invasion and immune suppression.^{46,47}

In addition, the remodeling of the microenvironment and stroma around PIA lesions, which can be quite extensive throughout the peripheral zone and other regions of the prostate, could also be fertile ground for pre-existing infiltrating adenocarcinoma cells. For example, as they migrate into these regions, tumor cells may co-opt the pre-existing FAP for neoplastic progression. This suggests that some of what is considered “reactive stroma” in cancer, with cancer associated fibroblasts (CAFs), may actually represent pre-existing altered stroma occurring in the pre-cancer microenvironment that may be encountered by, and at times co-opted by, the tumor cells. However, in some lesions, prostatic carcinomas occupy relatively large areas with no intermingling of benign glands. In these lesions, it is likely that the extent of FAP present indicates new expression in reactive tumor stroma that was not necessarily preexisting. This could occur either through activation of tissue-resident fibroblasts leading to FAP upregulation, in part through TGF- β signaling^{12,48} or through recruitment of mesenchymal precursors from systemic sources like the bone marrow.^{35,49,50}

CAFs have been widely studied and are often considered part of the “reactive stroma,” which in prostate cancer has been associated with aggressive disease and poor outcomes.^{51–54} In the present study, we found that the extent of FAP expression in the tumor microenvironment correlates with the presence of reactive stroma, which has been previously reported in a small series of cases.⁴⁸ This suggests that perhaps part of the association with reactive stroma with aggressive disease may relate to the presence of FAP overexpression. We also found that FAP levels were very low in grade group 1 tumors, but otherwise were not tightly associated with increasing grade group. However, FAP levels were associated with increased prostate cancer stage, which is an established marker of prostate cancer aggressiveness.

Prior studies have associated FAP with M2 macrophage infiltration.^{16,44,55–57} In the present study, the extent of FAP expression correlated with the extent of tumor infiltration by CD163 positive macrophages, which we verified were themselves higher in carcinoma than in normal appearing regions.⁴² Since these CD163-positive M2 macrophages are generally considered immunosuppressive, these findings are consistent with the hypothesis that FAP may contribute to immune suppression in the prostate tumor microenvironment.^{12,35,58,59} Interestingly, while FAP expression tended to occur in regions of inflammation, FAP expression did not correlate with overall CD45+ leukocyte density, suggesting some specificity of FAP and macrophage colocalization.

Our study has a number of limitations. First, we probed a relatively small number of cases and we do not have clinical follow-up on the cases studied. Also, we do not know the molecular mechanisms for FAP overexpression in human prostate stroma, benign or malignant. A number of cytokines and growth factors have been implicated in driving FAP expression. One prominent candidate for induction of FAP is TGF- β ,^{12,48,60,61} although additional studies are required to determine if this mechanism is actively occurring in human prostate tissues.

INCREASED FAP IN PIA AND PROSTATE CANCER

Furthermore, while we have ruled out FAP expression by macrophages and CD45 positive immune cells in our study, we have not further characterized the presumptive fibroblasts expressing FAP. CAFs are phenotypically heterogeneous in terms of gene expression and function with recent studies also indicating a diversity of biological functions.^{53,62,63} Recent studies using single cell RNAseq have provided new information about heterogeneous subtypes of cell states of fibroblasts in the tumor microenvironment of the prostate.^{17,32,64} Given this, it will be important to better define their phenotypes and localization spatially and quantitatively in non-neoplastic and neoplastic prostatic lesions. Future studies including additional multiplex IHC panels and *in situ* transcriptomics can help provide clarity to these questions.

Acknowledgments

We thank Dr Charles J. Bieberich for careful reading of the manuscript and helpful insight. This work is supported by NIH/NCI U54 CA274370 (AMDM and SY) NIH/ National Cancer Institute (NCI) Specialized Programs of Research Excellence (SPORE) in Prostate Cancer grant P50CA58236 (AMDM), NIH/NCI grant U01 CA196390 (AMDM and SY), R01 CA255259-04(WNB), R01 CA279993-01A1 (WNB), U.S. Department of Defense Prostate Cancer Research Program (PCRP), W81XWH-18-2-0015 (AMDM), NIH/NIBIB P41 EB024495 (MP), The Johns Hopkins Sidney Kimmel Comprehensive Cancer Center Oncology Tissue Services Laboratory is supported by NIH/NCI grant P30 CA006973 and The Patrick C. Walsh Prostate Cancer Research Fund at Johns Hopkins (AMDM and SY).

Financial Disclosure and Conflicts of Interest

AMDM is a paid consultant/advisor to Merck and Cepheid and has received research funding from Janssen and Myriad. SY receives research funding to his institution from Bristol-Myers Squibb and Celgene, Janssen, and Cepheid and has served as a consultant for Cepheid. He owns founder's equity in Brahm Astra Therapeutics and Digital Harmonic. MCM is a paid consultant to Clovis and Exelixis. WNB has received a monetary gift from Imago Biosciences, a subsidiary of Merck & Co., Inc.; sponsored research funding from Transcenta Holding, and owns founder's equity in ABIDA Bio, LLC

INCREASED FAP IN PIA AND PROSTATE CANCER

Table 1. Grade Group and Stage at Prostatectomy.

Grade Group	T2N0	T3N0	T3BN0/N1	Total
1	6	0	0	6
2	13	8	1	22
3	4	4	2	10
4	3	0	0	3
5	2	9	4	15
Total	28	21	7	56

INCREASED FAP IN PIA AND PROSTATE CANCER

Table 2. FAP area fraction (high and low thresholds) in random selected areas of normal appearing epithelium, PIA and Tumor

Case		Total FAP			High Threshold FAP		
		Normal	Carcinoma	PIA	Normal	Carcinoma	PIA
1	median	0.02853	0.093663	0.856993	0.005911	0.014668	0.23805
	mean	0.032737	0.1202954	1.491368	0.0058593	0.014329	0.423866
	SD	0.13157	0.668347	1.519038	0.005543	0.0085454	0.4955947
2	median	0.337393	1.735095	2.589456	0.032995	0.215894	0.504221
	mean	0.2862057	1.488986	3.330993	0.031131	0.2026046	0.9165356
	SD	0.1046561	1.078719	2.67103	0.0072939	0.1717262	0.8783959
3	median	0.833499	1.458605	1.68821	0.086693	0.136588	0.264828
	mean	0.8581937	1.356314	1.755053	0.935353	0.1619312	0.2577532
	SD	0.0473302	0.682906	0.7428295	0.0184263	0.1202342	0.134802
4	median	0.29669	0.445324	1.722643	0.002331	0.062162	0.338115
	mean	0.891427	1.285409	3.34904	0.0082647	0.2323456	1.460107
	SD	0.1094155	1.65396	4.041396	0.0108505	0.3471015	2.328966
5	median	0.01702	1.168963	1.193922	0.002163	0.18999	0.161467
	mean	0.17037	2.186287	1.396483	0.0025597	1.036728	0.4118354
	SD	0.113835	3.183496	1.657962	0.0021773	1.328368	0.6160603

INCREASED FAP IN PIA AND PROSTATE CANCER

Table 3a. Associations between variables (P values shown).

Variable		Grade			T2 vs > T2			N1 vs No N1			Tb3 vs <T3b		
		GG1	all others	<i>P</i>	T2	>T2	<i>P</i>	no N1	N1	<i>P</i>	<T3b	T3b	<i>P</i>
Tumor FAP Total	Median	1.21	1.71	0.44	2.36	3.39	0.09	1.69	4.65	0.05	1.73	3.72	0.13
	Range	3.49	8.14		9.63	13.1		8.16	10.8		8.16	11.22	
	SD	1.36	2.32		2.99	3.01		1.89	5.01		1.91	4.75	
FAP area fraction	Median	0.26	0.51	0.52	0.37	0.6	0.03	0.42	1.29	0.07	0.42	1.17	0.04
	Range	0.94	3.58		2.44	3.57		2.44	3.22		2.44	3.42	
	SD	0.36	0.69		0.6	0.71		0.53	1.54		0.53	1.4	
FAP stroma total	Median	0.38	0.77	0.33	2.36	3.39	0.09	2.59	6.59	0.04	2.63	5.4	0.07
	Range	1.38	3.96		9.63	13.1		9.63	10.78		9.63	11.9	
	SD	0.53	0.89		2.99	3.01		2.71	4.67		2.72	4.88	
FAP stroma fraction	Median	1.73	3.02	0.37	0.54	0.92	0.02	0.65	1.83	0.04	0.64	1.65	0.02
	Range	1.38	3.96		3.18	3.95		3.18	3.14		3.18	3.73	
	SD	5.09	13.16		0.84	0.86		0.76	1.43		0.76	1.38	
CD163 area fraction	Median	0.97	1.78	0.04	1.37	1.97	0.004	1.61	2.29	0.06	1.62	2.01	0.06
	Range	1.2	9.06		3.95	9.06		9.06	1.77		9.06	1.84	
	SD	0.4	1.37		1.05	1.52		1.35	0.73		1.37	0.72	
CD45 area fraction	Median	1.36	1.51	0.89	1.54	1.46	0.47	1.54	0.89	0.27	1.56	0.84	0.13
	Range	2.46	4.82		4.76	4.8		4.76	1.97		4.82	1.56	
	SD	0.9	1.21		1.11	1.27		1.19	0.94		1.21	0.64	

INCREASED FAP IN PIA AND PROSTATE CANCER

Table 3b. Associations between variables (P values shown).

Variable		Cribriform			Large Cribriform			IDCA			Reactive Stroma		
		absent	present	<i>P</i>	absent	present	<i>P</i>	absent	present	<i>P</i>	absent	present	<i>P</i>
Tumor FAP Total	Median	1.57	2.3	0.02	2.49	0.56	0.17	2.72	1.75	0.15	0.38	0.69	0.02
	Range	12.1	7.46		11.8	1.28		11.59	5.45		2.43	3.58	
	SD	2.57	1.92		2.67	0.56		2.58	1.79		0.52	0.81	
FAP area fraction	Median	0.35	0.64	0.01	0.25	0.63	0.04	0.42	0.5	0.33	0.34	0.69	0.02
	Range	3.58	2.43		1.37	1.75		1.39	3.58		2.44	3.58	
	SD	0.69	0.61		0.29	0.5		0.46	0.72		0.5	0.81	
FAP stroma total	Median	0.35	0.64	0.01	2.56	3.83	0.1	2.89	2.84	0.15	1.98	3.96	0.01
	Range	3.58	2.43		13.16	9.57		13.16	7.31		9.52	13.09	
	SD	0.69	0.61		3.06	2.75		3.15	2.64		2.35	3.46	
FAP stroma fraction	Median	2.04	3.85	0.002	0.61	1.08	0.02	0.74	0.7	0.26	0.48	1.03	0.01
	Range	13.16	9.57		3.96	2.79		3.96	1.86		3.18	3.96	
	SD	2.92	2.88		0.87	0.76		0.92	0.67		0.69	0.98	
CD163 area fraction	Median	0.46	1.04	0.02	1.52	2.05	0.78	1.62	1.76	0.38	1.68	1.65	0.18
	Range	3.96	3.17		3.95	9.06		9.06	3.26		9.06	3.15	
	SD	0.79	0.86		0.86	2.2		1.44	0.85		1.65	0.72	
CD45 area fraction	Median	1.62	1.76	0.71	1.47	1.57	0.91	1.63	1.05	0.87	1.69	1.16	0.05
	Range	9.06	3.26		4.76	4.68		4.76	3.11		4.74	4.8	
	SD	1.44	0.85		1.16	1.29		1.24	0.86		1.21	1.06	

INCREASED FAP IN PIA AND PROSTATE CANCER

Table 3c. Associations between variables (P values shown).

Variable		PTEN Any Loss			PTEN Homogenous Loss			ERG status		
		loss	retained	<i>P</i>	loss	retained	<i>P</i>	negative	positive	<i>P</i>
Tumor FAP Total	Median	2.45	1.71	0.15	2.7	1.77	0.29	1.85	2	0.81
	Range	5.41	12.1		5.41	12.1		8.16	12.06	
	SD	1.99	2.37		2.24	2.32		2.05	2.72	
FAP area fraction	Median	0.6	0.44	0.18	0.67	0.45	0.31	0.44	0.56	0.7
	Range	1.39	3.58		1.39	3.58		2.44	3.58	
	SD	0.52	0.69		0.58	0.67		0.57	0.81	
FAP stroma total	Median	3.55	2.6	0.21	4.08	1.77	0.35	2.9	2	0.95
	Range	7.27	13.16		7.27	12.1		9.63	12.06	
	SD	2.69	3.01		3.03	2.32		2.91	2.72	
FAP stroma fraction	Median	0.89	0.66	0.21	1.05	0.67	0.36	0.68	0.81	0.77
	Range	1.86	3.96		1.86	3.96		3.18	3.96	
	SD	0.7	0.87		0.78	0.84		0.8	0.97	
CD163 area fraction	Median	2.38	1.53	0.58	3.42	1.53	0.4	1.54	1.84	0.83
	Range	8.09	3.95		8.06	3.95		3.94	9.06	
	SD	2.59	0.93		3.82	0.9		0.92	1.83	
CD45 area fraction	Median	1.3	1.49	0.33	1.53	1.46	0.4	1.59	1.34	0.23
	Range	4.56	4.82		4.56	4.82		4.74	4.68	
	SD	1.44	1.13		2.16	1.1		1.16	1.22	

INCREASED FAP IN PIA AND PROSTATE CANCER

Supplemental Table 1. Antibodies, pretreatment and secondary antibody details and staining conditions.

Antigen	Source	Species	Clone	Dilution	Incubation Conditions	Antigen Retrieval	Secondary kit	Order in Panel
FAP	Abcam	rabbit	SP325	1:50	ON* 4C	EDTA	PowerVision+ (Leica PV6119)	1
p63	Cell Signaling	rabbit	D2K8X	1:500	45 min RT**	citrate	PowerVision+ (Leica PV6119)	2
CD163	BioSB	rabbit	EP324	1:100	45 min RT	citrate	PowerVision+ (Leica PV6119)	3
CD45	Cell Signaling	rabbit	D9M81	1:500	45 min RT	citrate	PowerVision+ (Leica PV6119)	4
CK8	Abcam	rabbit	EP1628Y	1:1000	45 min RT	citrate	PowerVision+ (Leica PV6119)	5

*ON: overnight, **RT: Room temperature

INCREASED FAP IN PIA AND PROSTATE CANCER

References:

1. Hamson EJ, Keane FM, Tholen S, Schilling O, Gorrell MD: Understanding fibroblast activation protein (FAP): substrates, activities, expression and targeting for cancer therapy. *Proteomics Clin Appl* [Internet] 2014, 8:454–463. Available from: <http://dx.doi.org/10.1002/prca.201300095>
2. Puré E, Blomberg R: Pro-tumorigenic roles of fibroblast activation protein in cancer: back to the basics. *Oncogene* [Internet] 2018, 37:4343–4357. Available from: <http://dx.doi.org/10.1038/s41388-018-0275-3>
3. Fitzgerald AA, Weiner LM: The role of fibroblast activation protein in health and malignancy. *Cancer Metastasis Rev* [Internet], Springer Science and Business Media LLC, 2020, 39:783–803. Available from: <http://dx.doi.org/10.1007/s10555-020-09909-3>
4. Rettig WJ, Garin-Chesa P, Beresford HR, Oettgen HF, Melamed MR, Old LJ: Cell-surface glycoproteins of human sarcomas: differential expression in normal and malignant tissues and cultured cells. *Proc Natl Acad Sci U S A* [Internet], Proceedings of the National Academy of Sciences, 1988, 85:3110–3114. Available from: <http://dx.doi.org/10.1073/pnas.85.9.3110>
5. Ramirez-Montagut T, Blachere NE, Sviderskaya EV, Bennett DC, Rettig WJ, Garin-Chesa P, Houghton AN: FAPalpha, a surface peptidase expressed during wound healing, is a tumor suppressor. *Oncogene* [Internet], Springer Science and Business Media LLC, 2004 [cited 2022 Mar 3], 23:5435–5446. Available from: <https://www.nature.com/articles/1207730>
6. Yang X, Lin Y, Shi Y, Li B, Liu W, Yin W, Dang Y, Chu Y, Fan J, He R: FAP Promotes

INCREASED FAP IN PIA AND PROSTATE CANCER

Immunosuppression by Cancer-Associated Fibroblasts in the Tumor Microenvironment via STAT3-CCL2 Signaling. *Cancer Res* [Internet] 2016, 76:4124–4135. Available from:

<http://dx.doi.org/10.1158/0008-5472.CAN-15-2973>

7. Kratochwil C, Flechsig P, Lindner T, Abderrahim L, Altmann A, Mier W, Adeberg S, Rathke H, Röhrich M, Winter H, Plinkert PK, Marme F, Lang M, Kauczor H-U, Jäger D, Debus J, Haberkorn U, Giesel FL: 68Ga-FAPI PET/CT: Tracer Uptake in 28 Different Kinds of Cancer. *J Nucl Med* [Internet] 2019, 60:801–805. Available from:
<http://dx.doi.org/10.2967/jnumed.119.227967>
8. Slania SL, Das D, Lisok A, Du Y, Jiang Z, Mease RC, Rowe SP, Nimmagadda S, Yang X, Pomper MG: Imaging of fibroblast activation protein in cancer xenografts using novel (4-quinolinoyl)-glycyl-2-cyanopyrrolidine-based small molecules. *J Med Chem* [Internet], American Chemical Society (ACS), 2021, 64:4059–4070. Available from:
<http://dx.doi.org/10.1021/acs.jmedchem.0c02171>
9. Kessel K, Seifert R, Weckesser M, Boegemann M, Huss S, Kratochwil C, Haberkorn U, Giesel F, Rahbar K: Prostate-specific membrane antigen and fibroblast activation protein distribution in prostate cancer: preliminary data on immunohistochemistry and PET imaging. *Ann Nucl Med* [Internet] 2021, . Available from: <http://dx.doi.org/10.1007/s12149-021-01702-8>
10. Nathaniel Brennen W, Isaacs JT, Denmeade SR: Rationale Behind Targeting Fibroblast Activation Protein–Expressing Carcinoma-Associated Fibroblasts as a Novel Chemotherapeutic Strategy. *Mol Cancer Ther* [Internet], American Association for Cancer Research, 2012 [cited 2021 Nov 1], 11:257–266. Available from:
<https://mct.aacrjournals.org/content/11/2/257.short>

INCREASED FAP IN PIA AND PROSTATE CANCER

11. Brennen WN, Rosen DM, Wang H, Isaacs JT, Denmeade SR: Targeting carcinoma-associated fibroblasts within the tumor stroma with a fibroblast activation protein-activated prodrug. *J Natl Cancer Inst* [Internet], Oxford University Press (OUP), 2012, 104:1320–1334. Available from: <https://academic.oup.com/jnci/article-lookup/doi/10.1093/jnci/djs336>
12. Brennen WN, J Thorek DL, Jiang W, Krueger TE, Antony L, Denmeade SR, Isaacs JT: Overcoming stromal barriers to immuno-oncological responses via fibroblast activation protein-targeted therapy. *Immunotherapy* [Internet] 2021, 13:155–175. Available from: <http://dx.doi.org/10.2217/imt-2020-0066>
13. Hintz HM, Gallant JP, Vander Griend DJ, Coleman IM, Nelson PS, LeBeau AM: Imaging Fibroblast Activation Protein Alpha Improves Diagnosis of Metastatic Prostate Cancer with Positron Emission Tomography. *Clin Cancer Res* [Internet] 2020, 26:4882–4891. Available from: <http://dx.doi.org/10.1158/1078-0432.CCR-20-1358>
14. Kesch C, Yirga L, Dendl K, Handke A, Darr C, Krafft U, Radtke JP, Tschirdewahn S, Szarvas T, Fazli L, Gleave M, Giesel FL, Haberkorn U, Hadaschik B: High fibroblast-activation-protein expression in castration-resistant prostate cancer supports the use of FAPI-molecular theranostics. *Eur J Nucl Med Mol Imaging* [Internet], Springer Science and Business Media LLC, 2021, . Available from: <http://dx.doi.org/10.1007/s00259-021-05423-y>
15. Hesterberg AB, Rios BL, Wolf EM, Tubbs C, Wong HY, Schaffer KR, Lotan TL, Giannico GA, Gordetsky JB, Hurley PJ: A distinct repertoire of cancer-associated fibroblasts is enriched in cribriform prostate cancer. *J Pathol Clin Res* [Internet], Wiley, 2021, . Available from: <http://dx.doi.org/10.1002/cjp2.205>
16. Pellinen T, Sandeman K, Blom S, Turkki R, Hemmes A, Välimäki K, Eineluoto J, Kenttämies A, Nordling S, Kallioniemi O, Rannikko A, Mirtti T: Stromal FAP Expression is

INCREASED FAP IN PIA AND PROSTATE CANCER

Associated with MRI Visibility and Patient Survival in Prostate Cancer. *Cancer Research Communications* [Internet], American Association for Cancer Research, 2022 [cited 2022 Nov 4], 2:172–181. Available from: <https://aacrjournals.org/cancerrescommun/article-abstract/2/3/172/694060>

17. Wong HY, Sheng Q, Hesterberg AB, Croessmann S, Rios BL, Giri K, Jackson J, Miranda AX, Watkins E, Schaffer KR, Donahue M, Winkler E, Penson DF, Smith JA, Herrell SD, Luckenbaugh AN, Barocas DA, Kim YJ, Graves D, Giannico GA, Rathmell JC, Park BH, Gordetsky JB, Hurley PJ: Single cell analysis of cribriform prostate cancer reveals cell intrinsic and tumor microenvironmental pathways of aggressive disease. *Nat Commun* [Internet], Springer Science and Business Media LLC, 2022 [cited 2022 Oct 17], 13:6036. Available from: <https://www.nature.com/articles/s41467-022-33780-1>
18. De Marzo AM, Platz EA, Sutcliffe S, Xu J, Grönberg H, Drake CG, Nakai Y, Isaacs WB, Nelson WG: Inflammation in prostate carcinogenesis. *Nat Rev Cancer* [Internet] 2007, 7:256–269. Available from: <http://dx.doi.org/10.1038/nrc2090>
19. Sfanos KS, Yegnasubramanian S, Nelson WG, De Marzo AM: The inflammatory microenvironment and microbiome in prostate cancer development. *Nat Rev Urol* [Internet] 2017, . Available from: <http://dx.doi.org/10.1038/nrurol.2017.167>
20. Nelson WG, Brawley OW, Isaacs WB, Platz EA, Yegnasubramanian S, Sfanos KS, Lotan TL, De Marzo AM: Health inequity drives disease biology to create disparities in prostate cancer outcomes. *J Clin Invest* [Internet], The American Society for Clinical Investigation, 2022, 132. Available from: <https://www.jci.org/articles/view/155031>
21. De Marzo AM, Marchi VL, Epstein JI, Nelson WG: Proliferative inflammatory atrophy of the prostate: implications for prostatic carcinogenesis. *Am J Pathol* [Internet] 1999, 155:1985–

INCREASED FAP IN PIA AND PROSTATE CANCER

1992. Available from: [http://dx.doi.org/10.1016/S0002-9440\(10\)65517-4](http://dx.doi.org/10.1016/S0002-9440(10)65517-4)
22. Parsons JK, Nelson CP, Gage WR, Nelson WG, Kensler TW, De Marzo AM: GSTA1 expression in normal, preneoplastic, and neoplastic human prostate tissue. *Prostate* [Internet], Wiley Online Library, 2001, 49:30–37. Available from: <https://www.ncbi.nlm.nih.gov/pubmed/11550208>
23. van Leenders GJLH, Gage WR, Hicks JL, van Balken B, Aalders TW, Schalken JA, De Marzo AM: Intermediate cells in human prostate epithelium are enriched in proliferative inflammatory atrophy. *Am J Pathol* [Internet], Elsevier, 2003, 162:1529–1537. Available from: [http://dx.doi.org/10.1016/S0002-9440\(10\)64286-1](http://dx.doi.org/10.1016/S0002-9440(10)64286-1)
24. Zha S, Gage WR, Sauvageot J, Saria EA, Putzi MJ, Ewing CM, Faith DA, Nelson WG, De Marzo AM, Isaacs WB: Cyclooxygenase-2 is up-regulated in proliferative inflammatory atrophy of the prostate, but not in prostate carcinoma. *Cancer Res* [Internet] 2001, 61:8617–8623. Available from: <https://aacrjournals.org/cancerres/article-abstract/61/24/8617/508255>
25. Wang W, Bergh A, Damber J-E: Increased expression of CCAAT/enhancer-binding protein beta in proliferative inflammatory atrophy of the prostate: relation with the expression of COX-2, the androgen receptor, and presence of focal chronic inflammation. *Prostate* [Internet] 2007, 67:1238–1246. Available from: <http://dx.doi.org/10.1002/pros.20595>
26. Sfanos KS, Wilson BA, De Marzo AM, Isaacs WB: Acute inflammatory proteins constitute the organic matrix of prostatic corpora amylacea and calculi in men with prostate cancer. *Proc Natl Acad Sci U S A* [Internet] 2009, 106:3443–3448. Available from: <http://dx.doi.org/10.1073/pnas.0810473106>
27. Liu X, Grogan TR, Hieronymus H, Hashimoto T, Mottahedeh J, Cheng D, Zhang L, Huang

INCREASED FAP IN PIA AND PROSTATE CANCER

- K, Stoyanova T, Park JW, Shkhyan RO, Nowroozizadeh B, Rettig MB, Sawyers CL, Elashoff D, Horvath S, Huang J, Witte ON, Goldstein AS: Low CD38 Identifies Progenitor-like Inflammation-Associated Luminal Cells that Can Initiate Human Prostate Cancer and Predict Poor Outcome. *Cell Rep* [Internet] 2016, 17:2596–2606. Available from: <http://dx.doi.org/10.1016/j.celrep.2016.11.010>
28. Nakayama M, Bennett CJ, Hicks JL, Epstein JI, Platz EA, Nelson WG, De Marzo AM: Hypermethylation of the human glutathione S-transferase-pi gene (GSTP1) CpG island is present in a subset of proliferative inflammatory atrophy lesions but not in normal or hyperplastic epithelium of the prostate: a detailed study using laser-capture microdissection. *Am J Pathol* [Internet] 2003, 163:923–933. Available from: <https://www.ncbi.nlm.nih.gov/pubmed/12937133>
29. Gupta H, Inoue H, Nakai Y, Nakayama M, Jones T, Hicks JL, Kumar B, Gurel M, Nelson WG, De Marzo AM, Yegnasubramanian S: Progressive spreading of DNA methylation in the GSTP1 promoter CpG island across transitions from precursors to invasive prostate cancer. *Cancer Prev Res* [Internet] 2023, . Available from: <http://dx.doi.org/10.1158/1940-6207.CAPR-22-0485>
30. Shrestha E, Coulter JB, Guzman W, Ozbek B, Hess MM, Mummert L, Ernst SE, Maynard JP, Meeker AK, Heaphy CM, Haffner MC, De Marzo AM, Sfanos KS: Oncogenic gene fusions in nonneoplastic precursors as evidence that bacterial infection can initiate prostate cancer. *Proc Natl Acad Sci U S A* [Internet], National Academy of Sciences, 2021 [cited 2021 Aug 2], 118. Available from: <https://www.pnas.org/content/118/32/e2018976118>
31. Huang FW, Song H, Weinstein HN, Xie J, Cooperberg MR, Hicks J, Mummert L, De Marzo AM, Sfanos KS: Club-like cells in proliferative inflammatory atrophy of the prostate. *J Pathol* [Internet] 2023, 261:85–95. Available from:

INCREASED FAP IN PIA AND PROSTATE CANCER

<https://pathsocjournals.onlinelibrary.wiley.com/doi/abs/10.1002/path.6149>

32. Graham MK, Wang R, Chikarmane R, Wodu B, Vaghasia A, Gupta A, Zheng Q, Hicks J, Sysa-Shah P, Pan X, Castagna N, Liu J, Meyers J, Skaist A, Zhang Y, Schuebel K, Simons B, Bieberich CJ, Nelson W, Lupold SE, DeWeese TL, De Marzo AM, Yegnasubramanian S: Convergent alterations in the tumor microenvironment of MYC-driven human and murine prostate cancer [Internet]. *bioRxiv*. 2023 [cited 2023 Sep 11], p. 2023.09.07.553268. Available from: <https://www.biorxiv.org/content/10.1101/2023.09.07.553268v1>
33. Ozbek B, Ertunc O, Erickson A, Vidal ID, Gomes-Alexandre C, Guner G, Hicks JL, Jones T, Taube JM, Sfanos KS, Yegnasubramanian S, De Marzo AM: Multiplex immunohistochemical phenotyping of T cells in primary prostate cancer. *Prostate* [Internet] 2022, . Available from: <http://dx.doi.org/10.1002/pros.24315>
34. Baena-Del Valle JA, Zheng Q, Hicks JL, Fedor H, Trock BJ, Morrissey C, Corey E, Cornish TC, Sfanos KS, De Marzo AM: Rapid Loss of RNA Detection by In Situ Hybridization in Stored Tissue Blocks and Preservation by Cold Storage of Unstained Slides. *Am J Clin Pathol* [Internet] 2017 [cited 2017 Oct 18], 148:398–415. Available from: <http://dx.doi.org/10.1093/ajcp/aqx094>
35. Brennen WN, Zhang B, Kulac I, Kisteman LN, Antony L, Wang H, Meeker AK, De Marzo AM, Garraway IP, Denmeade SR, Isaacs JT: Mesenchymal stem cell infiltration during neoplastic transformation of the human prostate. *Oncotarget* [Internet] 2017, 8:46710–46727. Available from: <http://dx.doi.org/10.18632/oncotarget.17362>
36. Salmon P, Oberholzer J, Occhiodoro T, Morel P, Lou J, Trono D: Reversible immortalization of human primary cells by lentivector-mediated transfer of specific genes. *Mol Ther* [Internet] 2000, 2:404–414. Available from:

INCREASED FAP IN PIA AND PROSTATE CANCER

<http://dx.doi.org/10.1006/mthe.2000.0141>

37. Graham MK, Principessa L, Antony L, Meeker AK, Isaacs JT: Low p16INK4a Expression in Early Passage Human Prostate Basal Epithelial Cells Enables Immortalization by Telomerase Expression Alone. *Prostate* [Internet] 2017, 77:374–384. Available from: <http://dx.doi.org/10.1002/pros.23276>
38. Sfanos KS, Yegnasubramanian S, Nelson WG, Lotan TL, Kulac I, Hicks JL, Zheng Q, Bieberich CJ, Haffner MC, De Marzo AM: If this is true, what does it imply? How end-user antibody validation facilitates insights into biology and disease. *Asian J Urol* [Internet] 2019, 6:10–25. Available from: <http://dx.doi.org/10.1016/j.ajur.2018.11.006>
39. Kregel S, Chen JL, Tom W, Krishnan V, Kach J, Brechka H, Fessenden TB, Isikbay M, Paner GP, Szmulewitz RZ, Vander Griend DJ: Acquired resistance to the second-generation androgen receptor antagonist enzalutamide in castration-resistant prostate cancer. *Oncotarget* [Internet] 2016, 7:26259–26274. Available from: <http://dx.doi.org/10.18632/oncotarget.8456>
40. Hintz HM, Cowan AE, Shapovalova M, LeBeau AM: Development of a Cross-Reactive Monoclonal Antibody for Detecting the Tumor Stroma. *Bioconjug Chem* [Internet] 2019, 30:1466–1476. Available from: <http://dx.doi.org/10.1021/acs.bioconjchem.9b00206>
41. Tsujikawa T, Kumar S, Borkar RN, Azimi V, Thibault G, Chang YH, Balter A, Kawashima R, Choe G, Sauer D, El Rassi E, Clayburgh DR, Kulesz-Martin MF, Lutz ER, Zheng L, Jaffee EM, Leyshock P, Margolin AA, Mori M, Gray JW, Flint PW, Coussens LM: Quantitative Multiplex Immunohistochemistry Reveals Myeloid-Inflamed Tumor-Immune Complexity Associated with Poor Prognosis. *Cell Rep* [Internet] 2017, 19:203–217. Available from: <http://dx.doi.org/10.1016/j.celrep.2017.03.037>

INCREASED FAP IN PIA AND PROSTATE CANCER

42. Zarif JC, Baena-Del Valle JA, Hicks JL, Heaphy CM, Vidal I, Luo J, Lotan TL, Hooper JE, Isaacs WB, Pienta KJ, De Marzo AM: Mannose Receptor-positive Macrophage Infiltration Correlates with Prostate Cancer Onset and Metastatic Castration-resistant Disease. *Eur Urol Oncol* [Internet] 2019, 2:429–436. Available from: <http://dx.doi.org/10.1016/j.euo.2018.09.014>
43. Chen J, Zheng Q, Hicks JL, Trabzonlu L, Ozbek B, Jones T, Vaghasia AM, Larman TC, Wang R, Markowski MC, Denmeade SR, Pienta KJ, Hruban RH, Antonarakis ES, Gupta A, Dang CV, Yegnasubramanian S, De Marzo AM: MYC-driven increases in mitochondrial DNA copy number occur early and persist throughout prostatic cancer progression. *JCI Insight* [Internet] 2023, 8. Available from: <http://dx.doi.org/10.1172/jci.insight.169868>
44. Cai J, Yang D, Sun H, Xiao L, Han F, Zhang M, Zhou L, Jiang M, Jiang Q, Li Y, Nie H: A multifactorial analysis of FAP to regulate gastrointestinal cancers progression. *Front Immunol* [Internet] 2023, 14:1183440. Available from: <http://dx.doi.org/10.3389/fimmu.2023.1183440>
45. Taylor BS, Schultz N, Hieronymus H, Gopalan A, Xiao Y, Carver BS, Arora VK, Kaushik P, Cerami E, Reva B, Antipin Y, Mitsiades N, Landers T, Dolgalev I, Major JE, Wilson M, Socci ND, Lash AE, Heguy A, Eastham JA, Scher HI, Reuter VE, Scardino PT, Sander C, Sawyers CL, Gerald WL: Integrative genomic profiling of human prostate cancer. *Cancer Cell* [Internet] 2010, 18:11–22. Available from: <http://dx.doi.org/10.1016/j.ccr.2010.05.026>
46. Kraman M, Bambrough PJ, Arnold JN, Roberts EW, Magiera L, Jones JO, Gopinathan A, Tuveson DA, Fearon DT: Suppression of antitumor immunity by stromal cells expressing fibroblast activation protein-alpha. *Science* [Internet] 2010, 330:827–830. Available from: <http://dx.doi.org/10.1126/science.1195300>

INCREASED FAP IN PIA AND PROSTATE CANCER

47. Joyce JA, Fearon DT: T cell exclusion, immune privilege, and the tumor microenvironment. *Science* [Internet] 2015, 348:74–80. Available from:
<http://dx.doi.org/10.1126/science.aaa6204>
48. Tuxhorn JA, Ayala GE, Smith MJ, Smith VC, Dang TD, Rowley DR: Reactive stroma in human prostate cancer: induction of myofibroblast phenotype and extracellular matrix remodeling. *Clin Cancer Res* [Internet] 2002, 8:2912–2923. Available from:
<https://www.ncbi.nlm.nih.gov/pubmed/12231536>
49. Bae S, Park CW, Son HK, Ju HK, Paik D, Jeon C-J, Koh GY, Kim J, Kim H: Fibroblast activation protein alpha identifies mesenchymal stromal cells from human bone marrow. *Br J Haematol* [Internet] 2008, 142:827–830. Available from: <http://dx.doi.org/10.1111/j.1365-2141.2008.07241.x>
50. Roberts EW, Deonaraine A, Jones JO, Denton AE, Feig C, Lyons SK, Espeli M, Kraman M, McKenna B, Wells RJB, Zhao Q, Caballero OL, Larder R, Coll AP, O’Rahilly S, Brindle KM, Teichmann SA, Tuveson DA, Fearon DT: Depletion of stromal cells expressing fibroblast activation protein- α from skeletal muscle and bone marrow results in cachexia and anemia. *J Exp Med* [Internet] 2013, 210:1137–1151. Available from:
<http://dx.doi.org/10.1084/jem.20122344>
51. Ayala GE, Muezzinoglu B, Hammerich KH, Frolov A, Liu H, Scardino PT, Li R, Sayeeduddin M, Ittmann MM, Kadmon D, Miles BJ, Wheeler TM, Rowley DR: Determining prostate cancer-specific death through quantification of stromogenic carcinoma area in prostatectomy specimens. *Am J Pathol* [Internet] 2011, 178:79–87. Available from:
<http://dx.doi.org/10.1016/j.ajpath.2010.09.042>
52. De Vivar AD, Sayeeduddin M, Rowley D, Cubilla A, Miles B, Kadmon D, Ayala G: Histologic

INCREASED FAP IN PIA AND PROSTATE CANCER

features of stromogenic carcinoma of the prostate (carcinomas with reactive stroma grade 3). *Hum Pathol* [Internet] 2017, 63:202–211. Available from: <http://dx.doi.org/10.1016/j.humpath.2017.02.019>

53. Blom S, Erickson A, Östman A, Rannikko A, Mirtti T, Kallioniemi O, Pellinen T: Fibroblast as a critical stromal cell type determining prognosis in prostate cancer. *Prostate* [Internet] 2019, 79:1505–1513. Available from: <http://dx.doi.org/10.1002/pros.23867>
54. Ruder S, Gao Y, Ding Y, Bu P, Miles B, De Marzo A, Wheeler T, McKenney JK, Auman H, Fazli L, Simko J, Hurtado-Coll A, Troyer DA, Carroll PR, Gleave M, Platz E, Trock B, Han M, Sayeeduddin M, True LD, Rowley D, Lin DW, Nelson PS, Thompson IM, Feng Z, Wei W, Brooks JD, Ittmann M, Lee M, Ayala G: Development and validation of a quantitative reactive stroma biomarker (qRS) for prostate cancer prognosis. *Hum Pathol* [Internet] 2022, 122:84–91. Available from: <http://dx.doi.org/10.1016/j.humpath.2022.01.009>
55. Zhou J, Wang X-H, Zhao Y-X, Chen C, Xu X-Y, Sun Q, Wu H-Y, Chen M, Sang J-F, Su L, Tang X-Q, Shi X-B, Zhang Y, Yu Q, Yao Y-Z, Zhang W-J: Cancer-Associated Fibroblasts Correlate with Tumor-Associated Macrophages Infiltration and Lymphatic Metastasis in Triple Negative Breast Cancer Patients. *J Cancer* [Internet] 2018, 9:4635–4641. Available from: <http://dx.doi.org/10.7150/jca.28583>
56. Ji D, Jia J, Cui X, Li Z, Wu A: FAP promotes metastasis and chemoresistance via regulating YAP1 and macrophages in mucinous colorectal adenocarcinoma. *iScience* [Internet] 2023, 26:106600. Available from: <http://dx.doi.org/10.1016/j.isci.2023.106600>
57. Yang A-T, Kim Y-O, Yan X-Z, Abe H, Aslam M, Park K-S, Zhao X-Y, Jia J-D, Klein T, You H, Schuppan D: Fibroblast Activation Protein Activates Macrophages and Promotes Parenchymal Liver Inflammation and Fibrosis. *Cell Mol Gastroenterol Hepatol* [Internet]

INCREASED FAP IN PIA AND PROSTATE CANCER

2023, 15:841–867. Available from: <http://dx.doi.org/10.1016/j.jcmgh.2022.12.005>

58. Krueger TE, Thorek DLJ, Meeker AK, Isaacs JT, Brennen WN: Tumor-infiltrating mesenchymal stem cells: Drivers of the immunosuppressive tumor microenvironment in prostate cancer? *Prostate* [Internet] 2019, 79:320–330. Available from: <http://dx.doi.org/10.1002/pros.23738>
59. Brennen WN, Denmeade SR, Isaacs JT: Mesenchymal stem cells as a vector for the inflammatory prostate microenvironment. *Endocr Relat Cancer* [Internet] 2013, 20:R269–R290. Available from: <http://dx.doi.org/10.1530/ERC-13-0151>
60. Krepela E, Vanickova Z, Hrabal P, Zubal M, Chmielova B, Balaziova E, Vymola P, Matrasova I, Busek P, Sedo A: Regulation of Fibroblast Activation Protein by Transforming Growth Factor Beta-1 in Glioblastoma Microenvironment. *Int J Mol Sci* [Internet] 2021, 22. Available from: <http://dx.doi.org/10.3390/ijms22031046>
61. Wu F, Yang J, Liu J, Wang Y, Mu J, Zeng Q, Deng S, Zhou H: Signaling pathways in cancer-associated fibroblasts and targeted therapy for cancer. *Signal Transduct Target Ther* [Internet] 2021, 6:218. Available from: <http://dx.doi.org/10.1038/s41392-021-00641-0>
62. Biffi G, Tuveson DA: Diversity and Biology of Cancer-Associated Fibroblasts. *Physiol Rev* [Internet] 2021, 101:147–176. Available from: <http://dx.doi.org/10.1152/physrev.00048.2019>
63. Owen JS, Clayton A, Pearson HB: Cancer-associated fibroblast heterogeneity, activation and function: Implications for prostate cancer. *Biomolecules* [Internet], Multidisciplinary Digital Publishing Institute, 2022 [cited 2023 Feb 11], 13:67. Available from: <https://www.mdpi.com/2218-273X/13/1/67>
64. Henry GH, Malewska A, Joseph DB, Malladi VS, Lee J, Torrealba J, Mauck RJ, Gahan JC, Raj GV, Roehrborn CG, Hon GC, MacConmara MP, Reese JC, Hutchinson RC, Vezina

INCREASED FAP IN PIA AND PROSTATE CANCER

CM, Strand DW: A Cellular Anatomy of the Normal Adult Human Prostate and Prostatic Urethra. *Cell Rep* [Internet] 2018, 25:3530–3542.e5. Available from: <http://dx.doi.org/10.1016/j.celrep.2018.11.086>

65. Abeshouse A, Ahn J, Akbani R, Ally A, Amin S, Andry CD, Annala M, Aprikian A, Armenia J, Arora A, Todd Auman J, Balasundaram M, Balu S, Barbieri CE, Bauer T, Benz CC, Bergeron A, Beroukhi R, Berrios M, Bivol A, Bodenheimer T, Boice L, Bootwalla MS, dos Reis RB, Boutros PC, Bowen J, Bowlby R, Boyd J, Bradley RK, Breggia A, Brimo F, Bristow CA, Brooks D, Broom BM, Bryce AH, Bublely G, Burks E, Butterfield YSN, Button M, Canes D, Carlotti CG, Carlsen R, Carmel M, Carroll PR, Carter SL, Cartun R, Carver BS, Chan JM, Chang MT, Chen Y, Cherniack AD, Chevalier S, Chin L, Cho J, Chu A, Chuah E, Chudamani S, Cibulskis K, Ciriello G, Clarke A, Cooperberg MR, Corcoran NM, Costello AJ, Cowan J, Crain D, Curley E, David K, Demchok JA, Demichelis F, Dhalla N, Dhir R, Doueik A, Drake B, Dvinge H, Dyakova N, Felau I, Ferguson ML, Frazer S, Freedland S, Fu Y, Gabriel SB, Gao J, Gardner J, Gastier-Foster JM, Gehlenborg N, Gerken M, Gerstein MB, Getz G, Godwin AK, Gopalan A, Graefen M, Graim K, Gribbin T, Guin R, Gupta M, Hadjipanayis A, Haider S, Hamel L, et al.: The Molecular Taxonomy of Primary Prostate Cancer. *Cell* [Internet], Elsevier, 2015 [cited 2020 Dec 9], 163:1011–1025. Available from: [https://www.cell.com/fulltext/S0092-8674\(15\)01339-2](https://www.cell.com/fulltext/S0092-8674(15)01339-2)

Figure Legends

Figure 1. Analytic validation of FAP IHC assay. (A) hPrCSC-44c cells were immortalized from hPrCSC-44c cells that are known to be positive for FAP mRNA and protein and showed robust positive staining. (B) Targeted disruption of FAP using CRISPR/Cas9 resulted in an absence of IHC staining. (C) EnzaR-CWR22Rv1 prostate cancer cells are known to be negative for FAP and stained negatively prior to transfection, but were strongly positive following transfection with a FAP cDNA clone (D).

Figure 2. Multiplex Chromogenic IHC assay showing FAP expression in tumor region. FAP expression is restricted to the tumor stromal compartment. (A) View of chromogenic stain of FAP in a region of a tumor in which malignant glands surround a benign acinus in the center. (B) Iterative chromogenic stain on the same slide stained for CD163 IHC staining (M2 macrophages) in the same area described in A. (C) Pseudocolored deconvoluted image of A showing FAP (yellow) and nuclei (blue). (D) Same view as in C but with the addition of CD163 in fuchsia. (E) Same view adding CK8 in white and p63 (basal cells) in cyan. (F) Same view adding CD45 (pan immune cell marker) in green.

Figure 3. FAP IHC staining in benign prostate regions. (A-B) Normal prostatic epithelium and stroma show absence of staining for FAP protein. (C-D) Strong positive staining for FAP is present in the stromal compartment of a PIA lesion showing mild to moderate chronic inflammation and corpora amylacea (CA). Blue arrow indicates positive FAP staining. Black arrows indicate mononuclear inflammatory cells in the stroma. (E-F) H&E staining shows a region of fibrosis (Fib) surrounding an atrophic gland in another region of PIA. Blue arrows indicate positive areas of FAP staining in the stroma. Black arrows indicate mononuclear immune cell infiltrates.

Figure 4. Marked heterogeneity of FAP in prostatic adenocarcinoma. (A) Region of invasive adenocarcinoma showing high levels of FAP staining in the tumor stromal compartment. (B) Another region from the same tumor has much less FAP staining. Black arrows indicate epithelial tumor cells and blue arrows indicate stromal regions staining positively for FAP.

Figure 5. Strongest FAP staining occurs near benign glands even more so than nearby positively staining tumor. (A) Low power view showing region of invasive adenocarcinoma (left) directly adjacent to benign PIA glands and stroma (region within dashed black line). Strongest staining for FAP (blue arrow) is around benign gland that contains corpora amylacea (CA). Black arrows indicate tumor epithelial cells. Blue arrows indicate positive FAP staining in stroma. (B) Higher power view of region in A outlined with the blue dashed line.

Figure 6. High levels of FAP occur around cribriform and intraductal lesions. Images show medium power view of chromogenic FAP staining (A and C) and p63 (B and D, highlighting nuclei of basal cells) of a high grade lesion with invasive adenocarcinoma (black arrows - invasive) and intraductal carcinoma (blue arrows - IDCA). Red arrows shows benign glands. Note strong FAP staining (*) in the stroma that is localized adjacent to epithelial tumor cell clusters.

INCREASED FAP IN PIA AND PROSTATE CANCER

Figure 7. Multiplex chromogenic IHC assay and image analysis pipeline showing FAP area quantification. FAP expression is restricted to the tumor stromal compartment. **A)** low power view of whole slide with area of tumor demarcated in yellow. **B)** Use of Random Forest Classifier to detect tumor epithelium (red), stroma (green), and gland lumens (black). **C)** higher power view of tumor with FAP (yellow), epithelium (white), and nuclei (blue). **D)** Automated image analysis detection of FAP for area quantification (red is strong intensity, orange is medium and yellow is low intensity). **E)** Same region as C and D showing Random Forest Classifier as in **B**. **F)** Markers used for panel 1 (CD45 (green-all immune cells), CD163 in fuchsia (M2 macrophages), FAP (yellow) and keratin 8 (white)).

Figure 8. FAP area fraction and paired analyses from different regions (normal, PIA and tumor) from matched patients. A-C). Quantification using the median value. Each point on the graph represents the median value from multiple regions from a given patient. Each color represents matched regions from the same patient.

Figure 9. Quantitative analysis of FAP, CD163 and CD45 in carcinoma by grade, stage and the presence of cribriform glands. A-C) Quantification by grade group. **D-F)** Quantification by pathological stage at prostatectomy (organ confined versus non organ confined status). **G-I)**, Quantification by the presence of cribriform glands in carcinoma.

Figure 10. FAP area fraction in carcinoma correlates with CD163 area fraction, but not with CD45 area fraction.

Supplemental Figure 1. FAP area fraction from all data points used for data shown in Fig. 8. A-C) Each color dot represents the FAP area fraction (percentage of area occupied by FAP staining) in a given region of interest in that tissue type, including all areas (multiple areas per patient) from all 5 patients. There is a marked increase of FAP in tumor and PIA regions.

Supplemental Figure 2. FAP mRNA expression data from The JHU LCM Prostatectomy Dataset⁴³, showing its expression in benign and adenocarcinoma regions (N= 114 patients with cancer and 120 patients with benign). TPM represents transcripts per million data.

Supplemental Figure 3. FAP expression in reactive stroma. A) H&E image of a region of prostatic adenocarcinoma showing reactive stroma between cancerous glands. **B)** FAP stained slide from an adjacent slide from the same region as in **A** showing intense staining in areas of reactive stroma. **C)** Same tumor in a different region, where there is no reactive stroma. **D)** FAP stained slide of the same view as **C**, showing low intense staining in areas lacking reactive stroma.

INCREASED FAP IN PIA AND PROSTATE CANCER

Supplemental Figure 4. Correlation between FAP mRNA and CD163 mRNA expression from RNAseq datasets. **A**, Data from MSKCC *Cancer Cell*⁴⁵ (N = 131 samples from primary tumors with mRNA). **B**, Data from Chen et al., Johns Hopkins, *JCI Insight*⁴³ (N = 126 samples from 120 patients) . **C**, Data from TCGA, *Cell*, 2015⁶⁵ (N = 290 samples/patients).

Supplemental Figure 5. Quantitative analysis of FAP, CD163 and CD45 in relation to common molecular alterations in prostate cancer. **A-F**) Quantitative analysis of FAP, CD163, and CD45 area fraction in cases with any (heterogeneous) PTEN loss (**A-C**) or homogeneous PTEN loss (**D-F**). **G-I**) Quantitative analysis of FAP area fraction in cases in relation to ERG status.

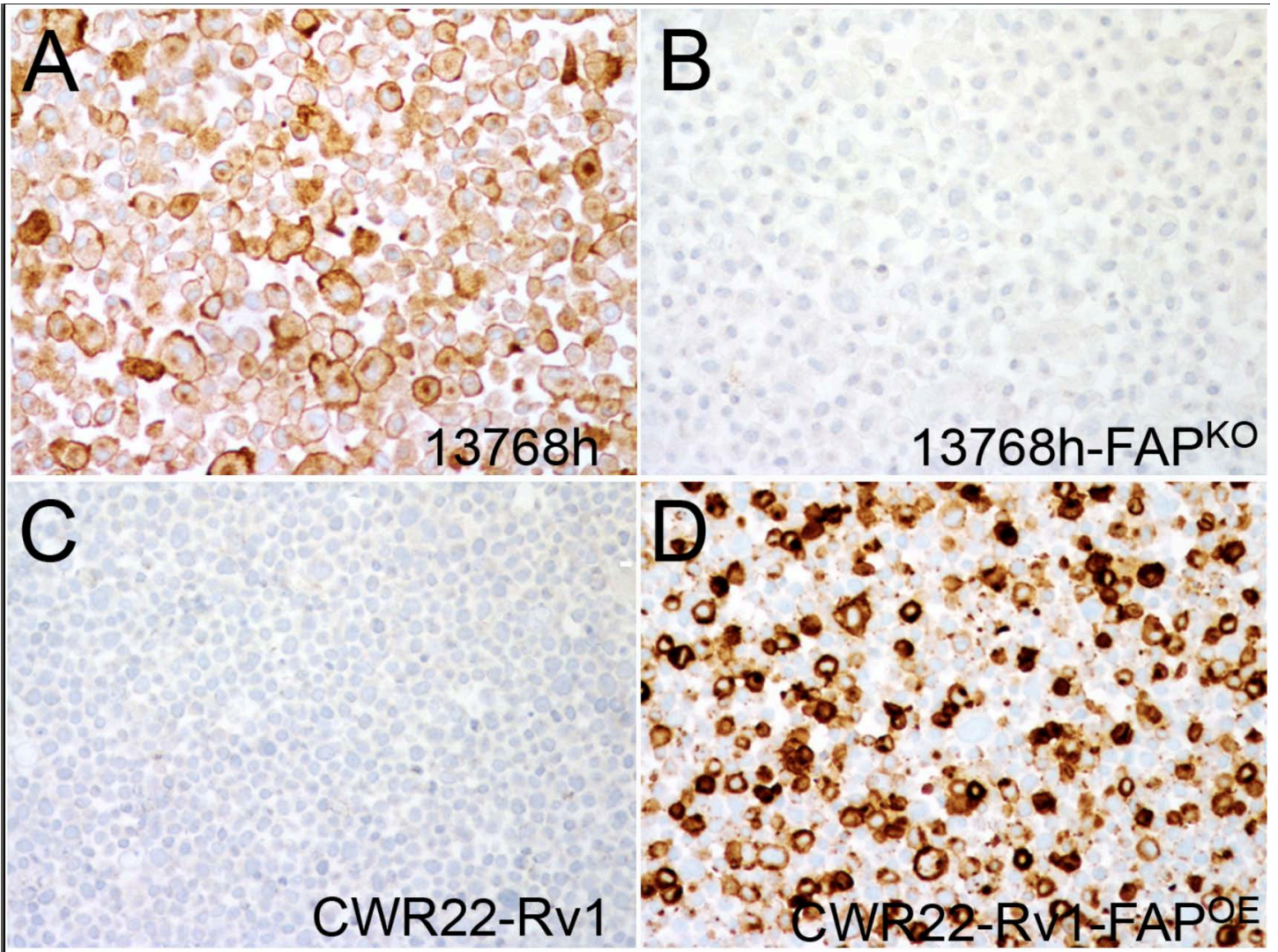


Figure 1. Analytic validation of FAP IHC assay.

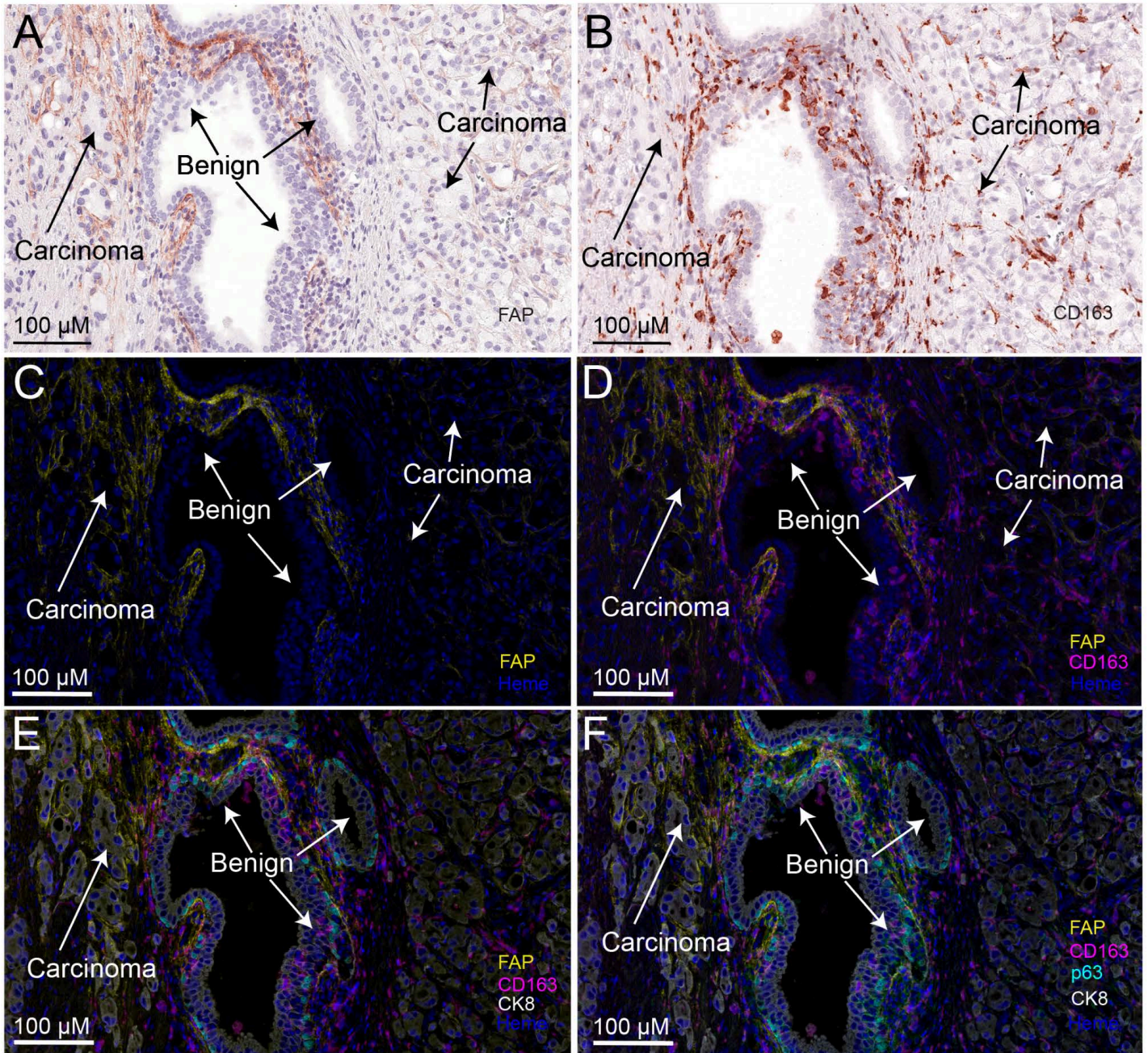


Figure 2. Multiplex Chromogenic IHC assay showing FAP expression in tumor region.

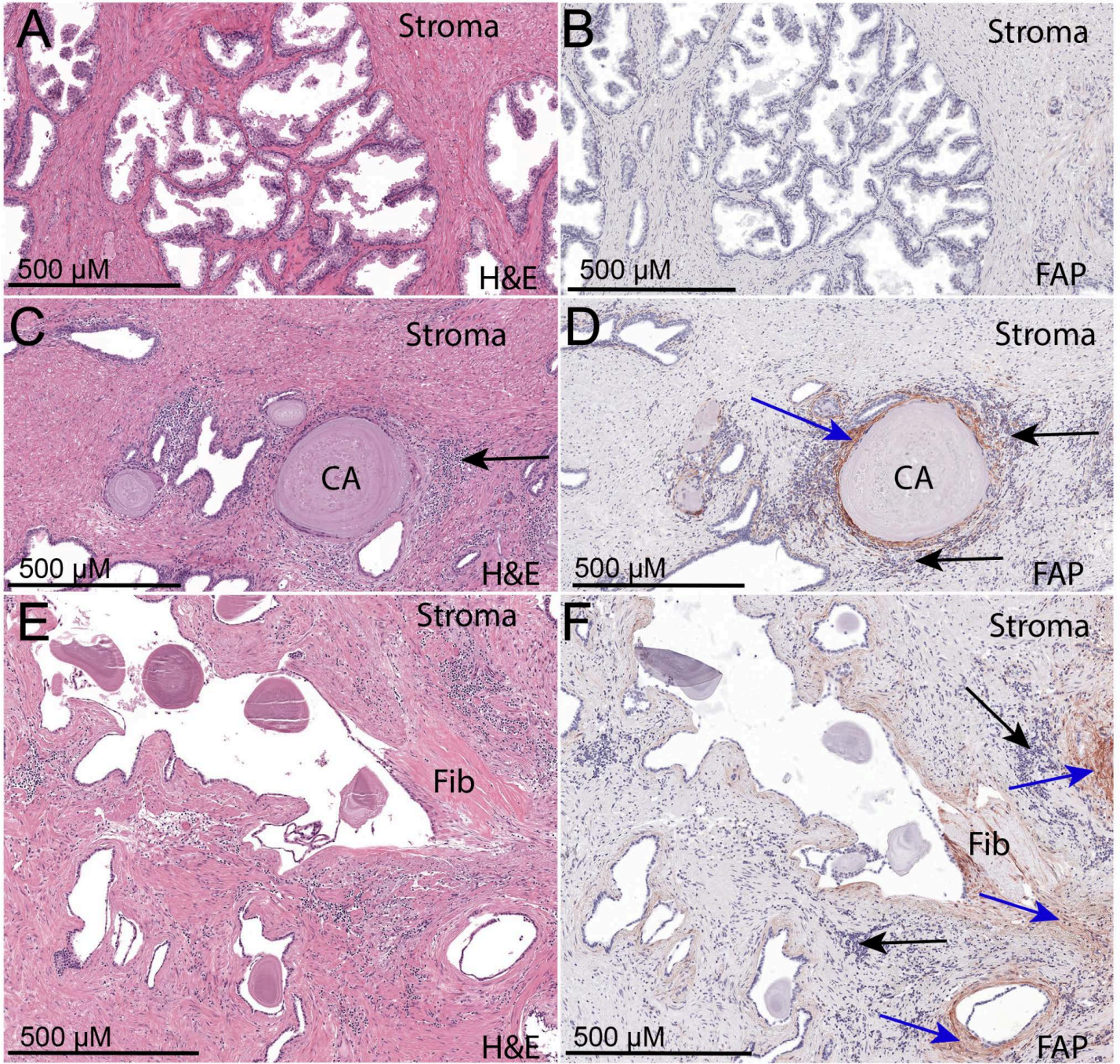


Figure 3. FAP IHC staining in benign prostate regions.

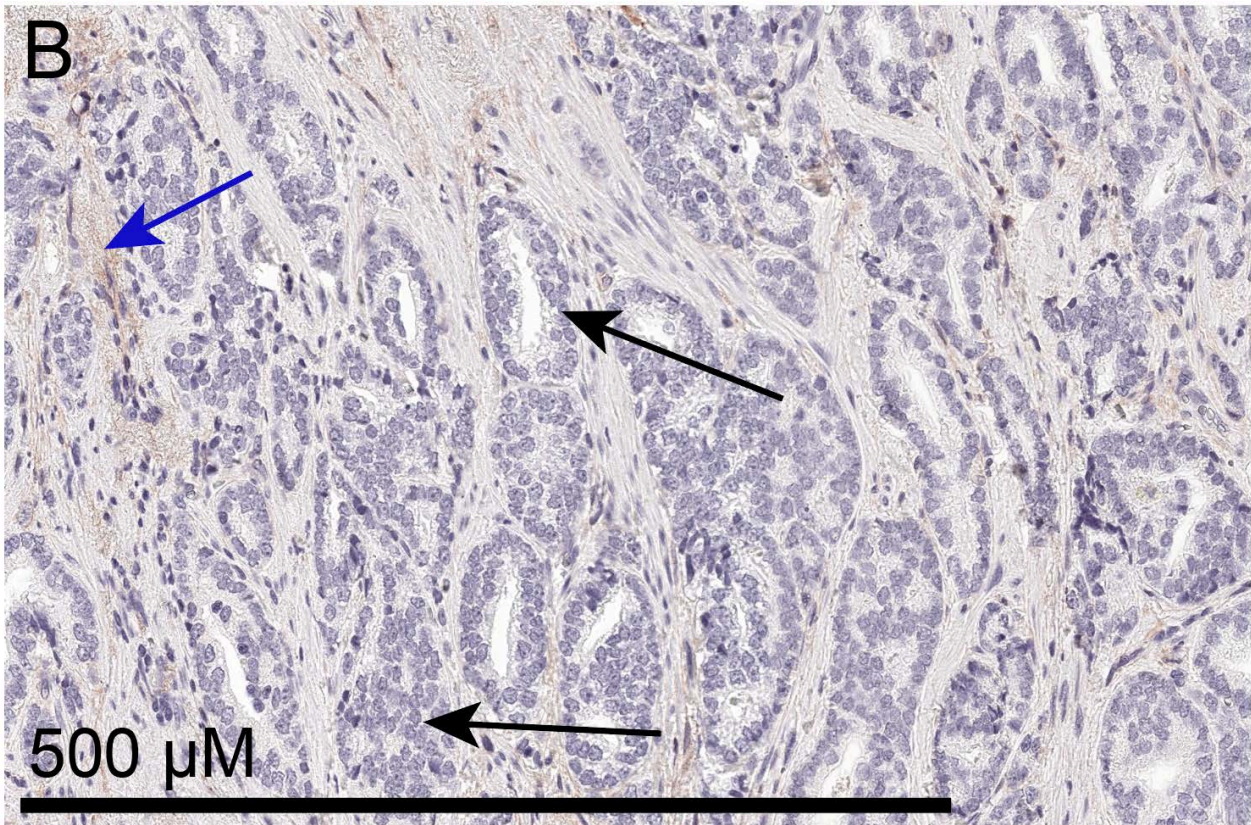
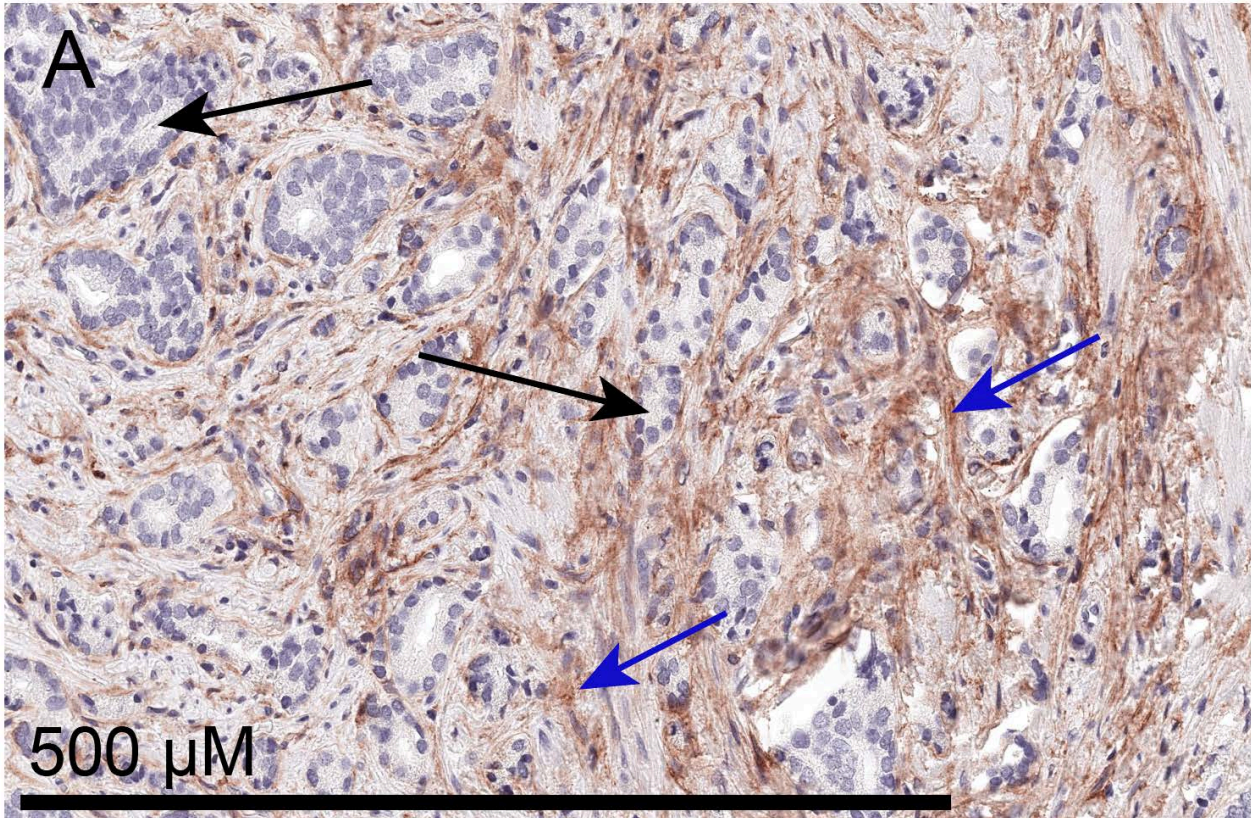


Figure 4. Marked heterogeneity of FAP in prostatic adenocarcinoma.

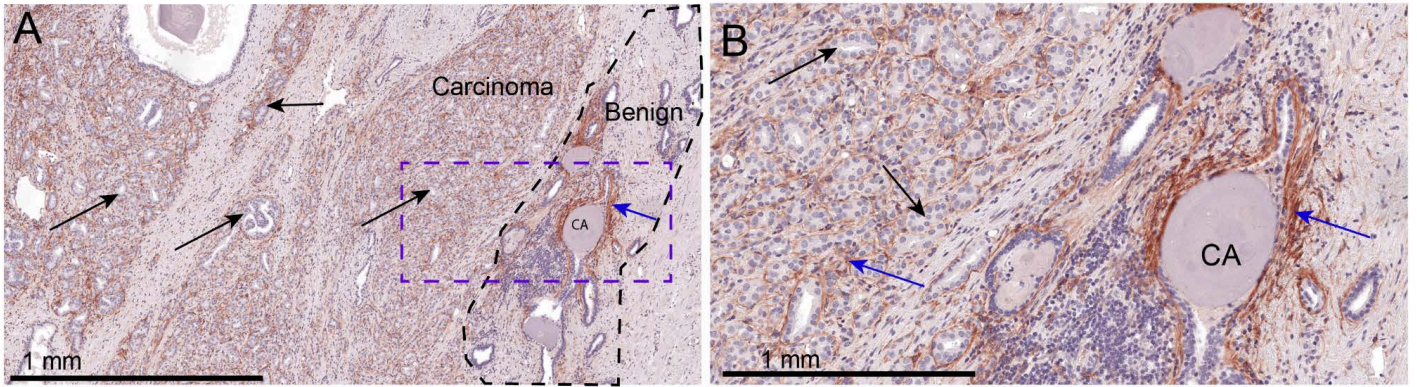


Figure 5. Strongest FAP staining occurs near benign glands even near positively staining tumor.

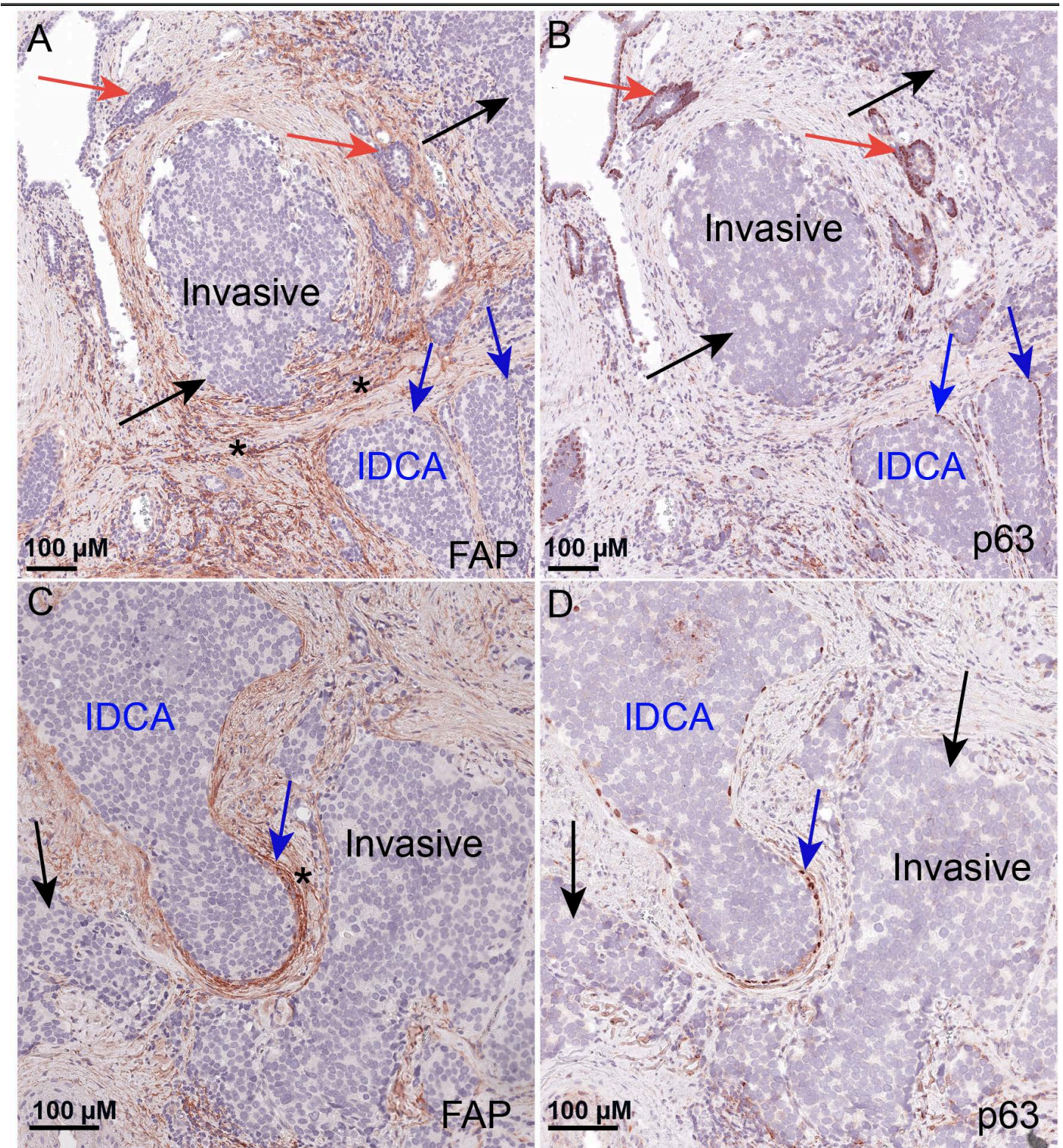


Figure 6. High levels of FAP occur around cribriform and intraductal lesions.

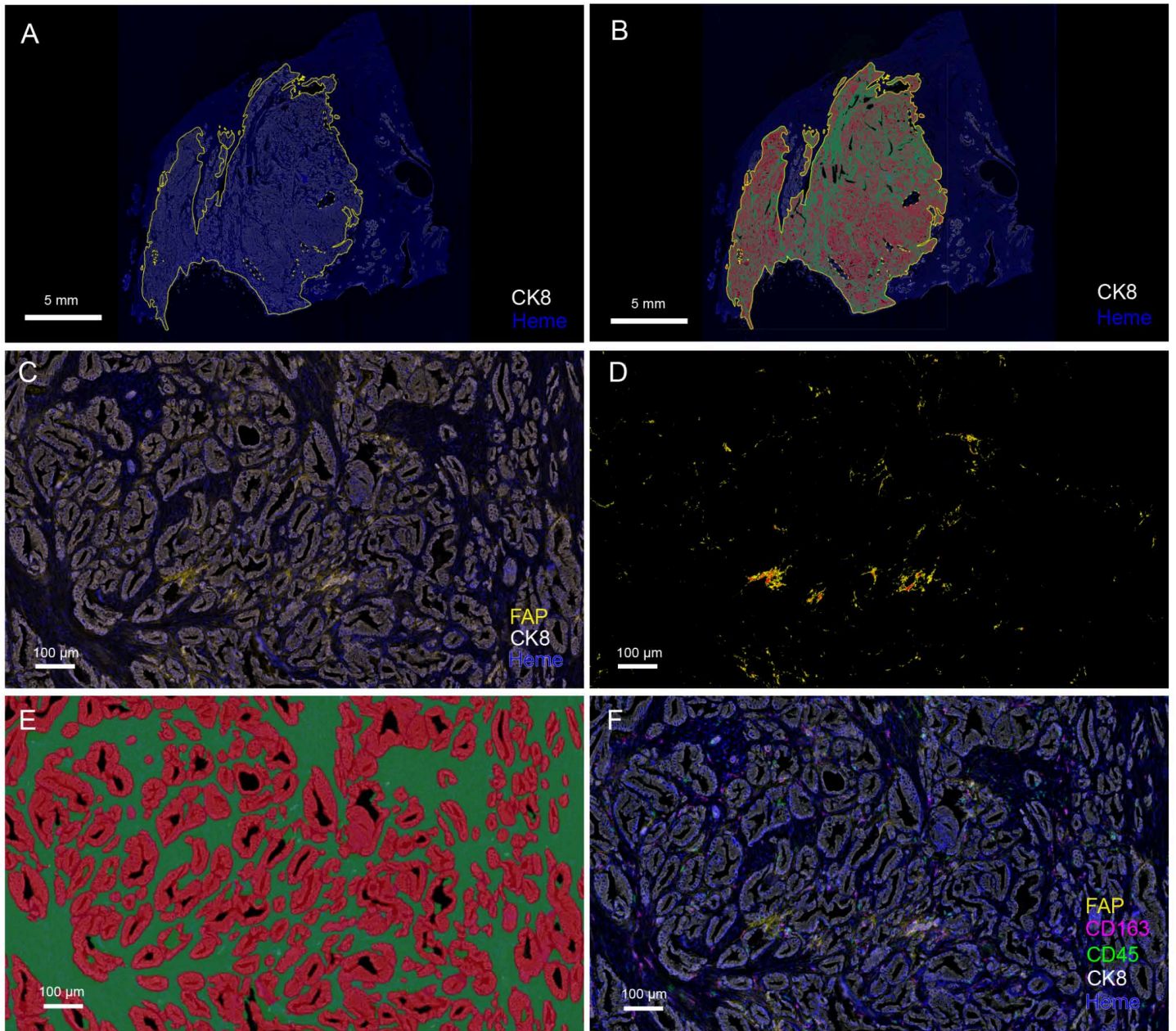


Figure 7. Multiplex chromogenic IHC assay and image analysis pipeline showing FAP area quantification.

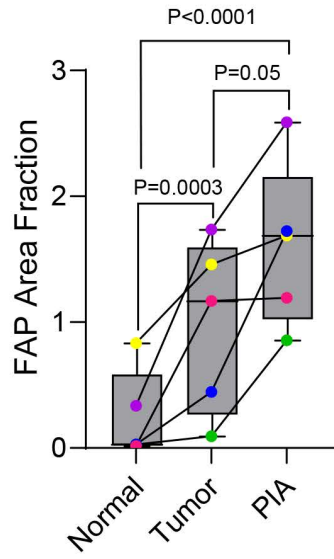
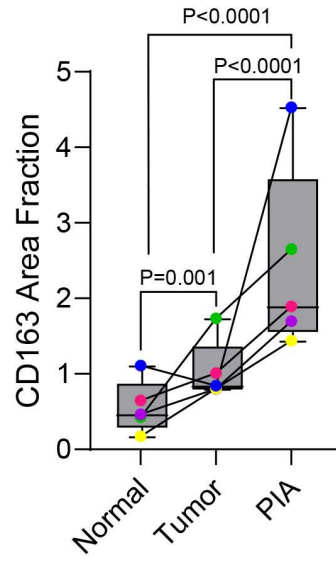
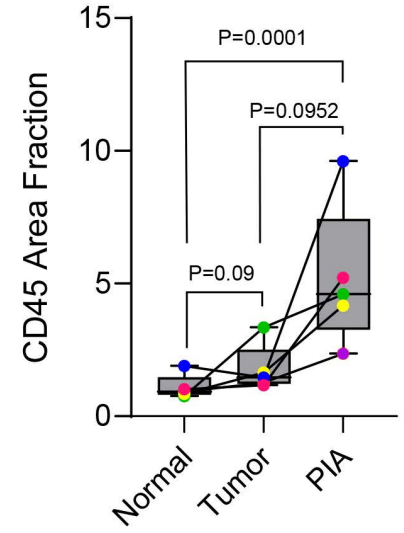
A**B****C**

Figure 8. FAP area fraction and paired analyzes from different regions (normal, PIA and tumor) from matched patients.

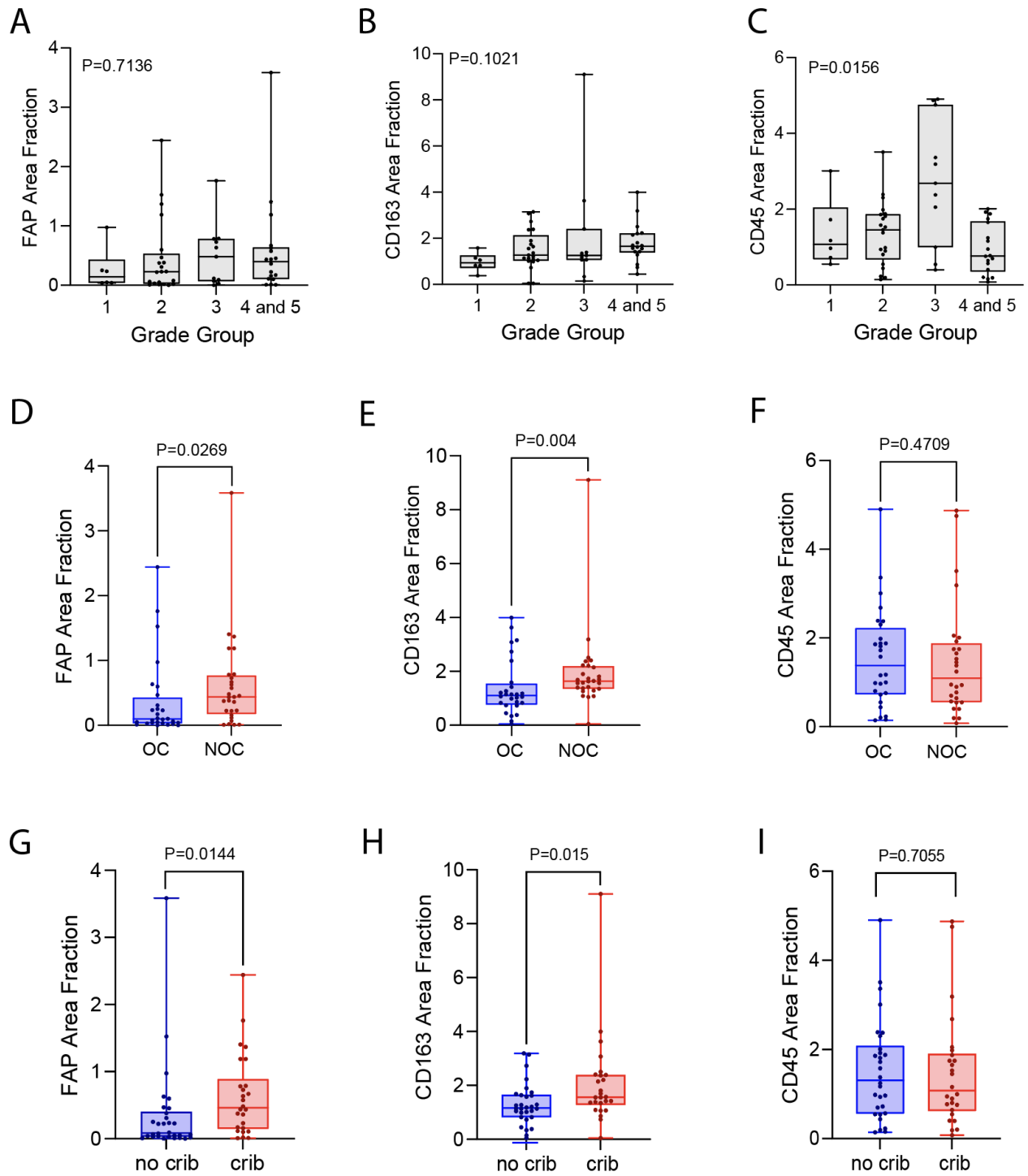


Figure 9. Quantitative analysis of FAP, CD163 and CD45 in carcinoma by grade, stage and the presence of cribriform glands.

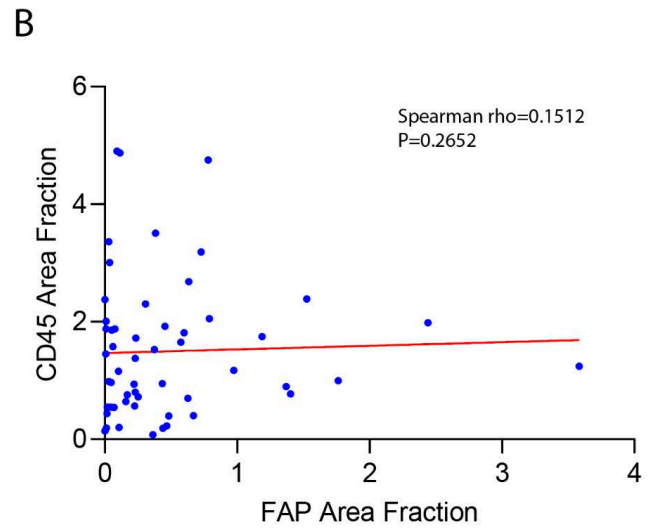
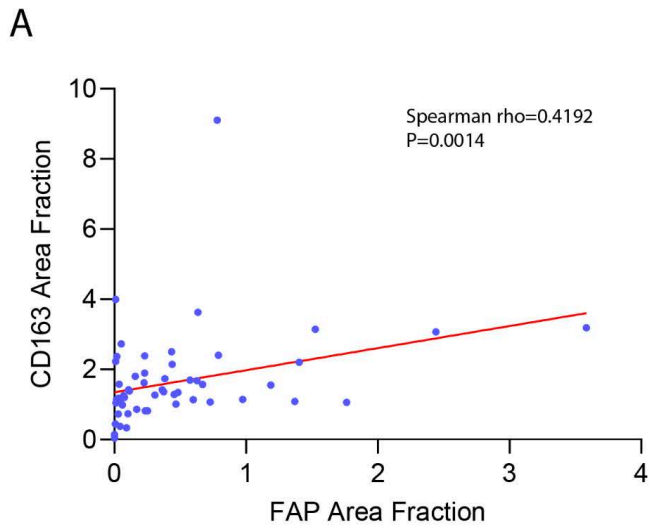
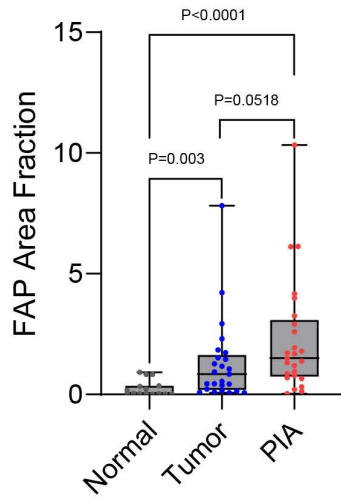
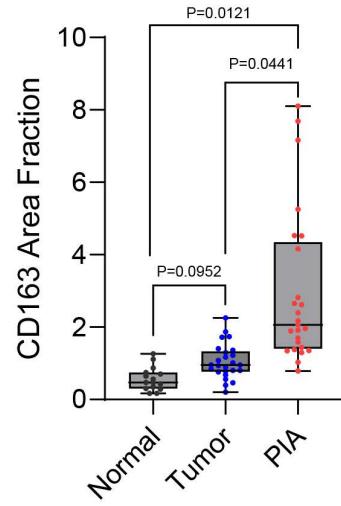
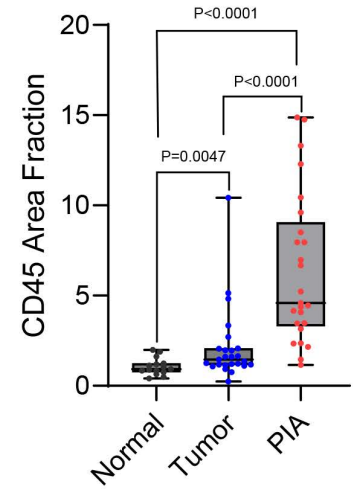
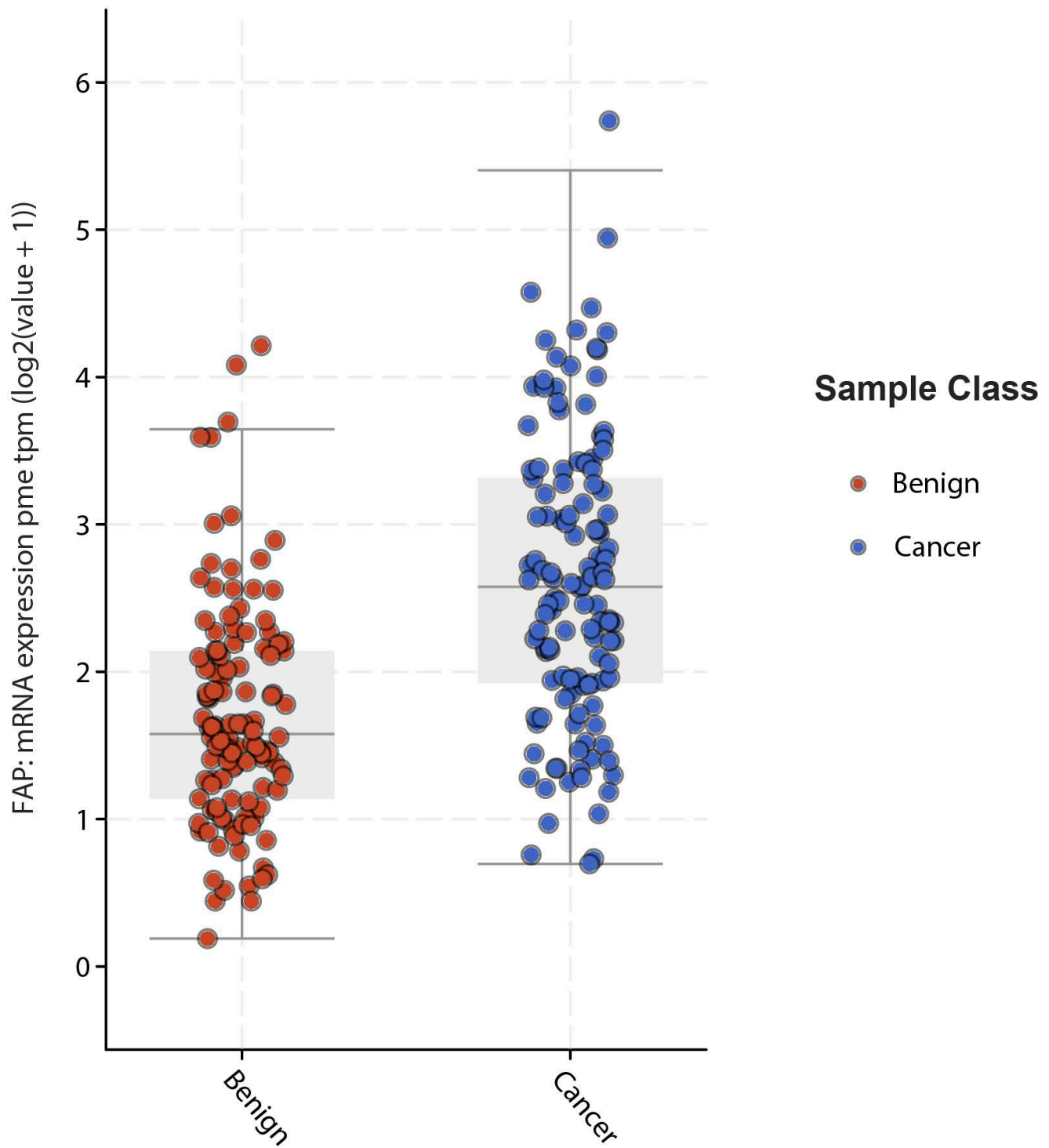


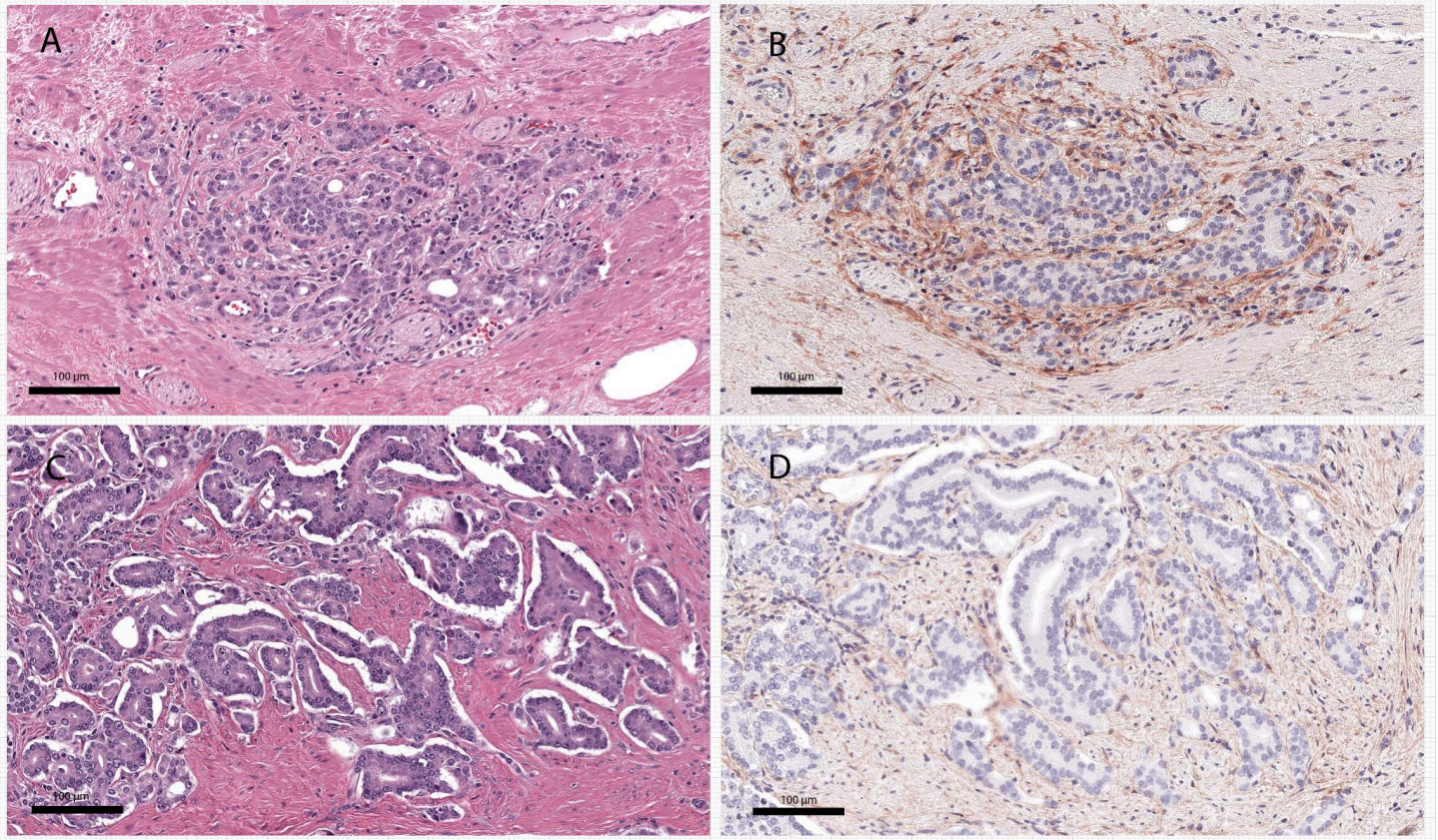
Figure 10. FAP area fraction in carcinoma correlates with CD163 area fraction, but not with CD45 area fraction.

A**B****C**

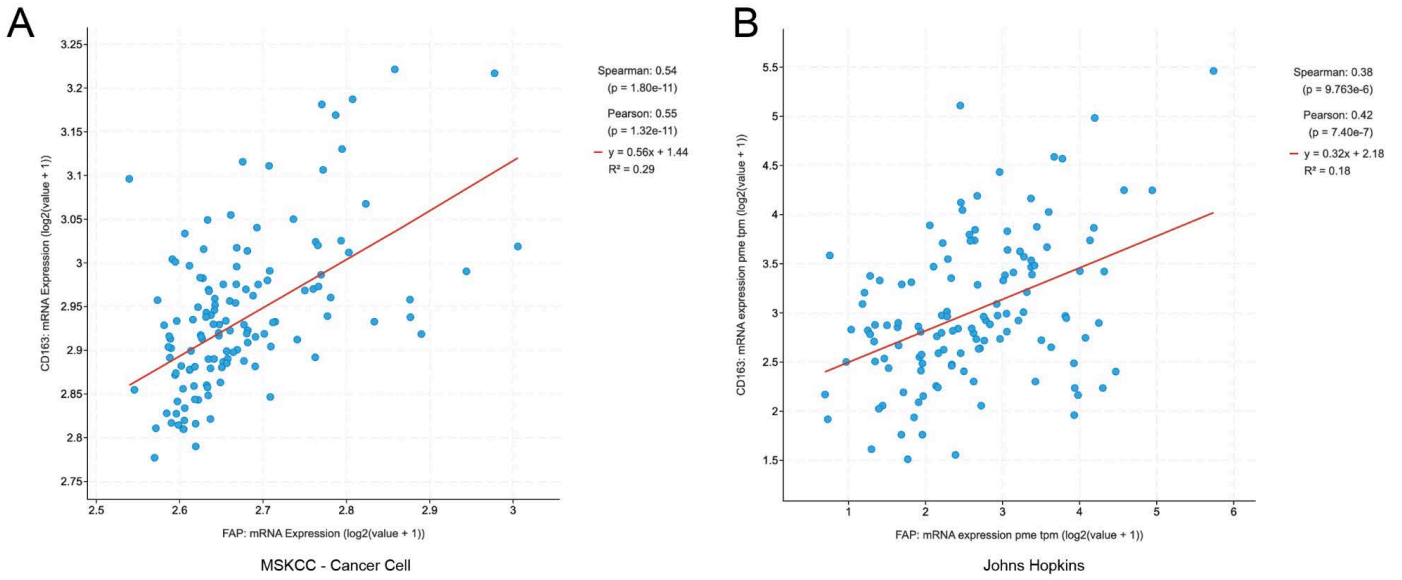
Supplemental Figure 1. FAP area fraction from all data points used for data shown in Fig. 8.



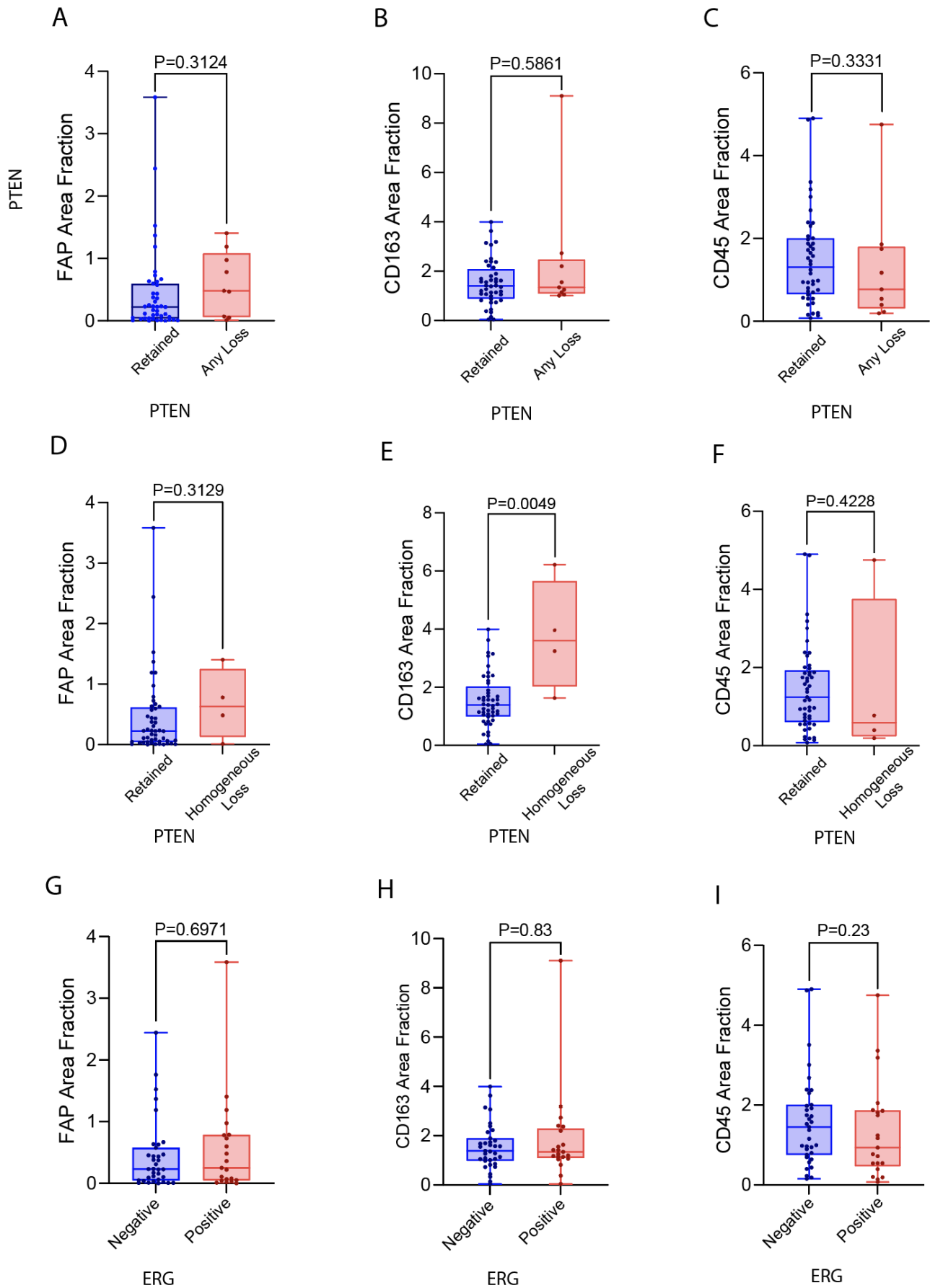
Supplemental Figure 2. FAP mRNA expression data from U01 dataset, showing its expression in benign and adenocarcinoma regions (N= 114 patients with cancer and 120 patients with benign). TPM represents transcripts per million data.



Supplemental Figure 3. FAP expression in reactive stroma.



Supplemental Figure 4. Correlation between FAP mRNA and CD163 mRNA expression from RNAseq datasets. A, Data from MSKCC *Cancer Cell* ([Taylor et al. 2010](#)). **B,** Data from Chen et al., Johns Hopkins *JCI Insight* ([Chen et al. 2023](#)).



Supplemental Figure 5. Quantitative analysis of FAP, CD163 and CD45 in relation to common molecular alterations in prostate cancer.

